Org. Geochem. Vol. 20, No. 8, pp. 1165–1186, 1993
Printed in Great Britain.

0146-6380/93 $6.00 + 0.00

A molecular stratigraphic approach to palaeoenvironmental assessment and the recognition of changes in source inputs in marls of the Mulhouse Basin (Alsace, France)

B. J. KEELY,[1]* J. S. SINNINGHE DAMSTÉ,[2]† S. E. BETTS,[2] LING YUE,[2] J. W. DE LEEUW,[2]† and J. R. MAXWELL[1]

[1]Organic Geochemistry Unit, University of Bristol, School of Chemistry, Cantock's Close, Bristol BS8 1TS, U.K. and [2]Organic Geochemistry Unit, Department of Chemical Technology and Materials Science, Delft University of Technology, De Vries van Heystplantsoen 2, 2628 RZ Delft, The Netherlands

Abstract—Principal components analysis (PCA) has been used to investigate changes in concentrations of the components of the hydrocarbon fractions extracted from 71 marl samples, selected to cover two total organic carbon (TOC) maxima in the lower part of the Salt IV formation, a Lower Oligocene evaporitic sequence from the Mulhouse Basin, France. The analysis indicates that the fractions can be ascribed as lying between two end member distributions. The changes in these distributions are gradual, suggesting that they resulted from fairly gradual changes in the depositional palaeoenvironment. These changes are related to increased algal productivity associated with the evolution of a restricted lacustrine environment through to one with a greater marine influence. Systematic variations in the concentrations of selected components relative to the TOC profile point to a repeated sequential evolution in the biological assemblage during deposition of the sequence.

Key words—palaeoenvironmental assessment, molecular stratigraphy, organic matter in marls, evaporite sequence, marine ingression, hydrocarbons in evaporites, principal components analysis

INTRODUCTION

Because of the paucity of fossil remains in many ancient evaporitic sedimentary sequences it was originally believed that the depositional environments in question were virtually devoid of life (e.g. Lotze, 1957). Consequently, the hydrocarbon source potential of such sequences was overlooked. It is now clear, however, that in these apparently hostile environments low species diversity is compensated by high numbers of individuals. Thus, studies of modern day evaporitic settings (e.g. saline lakes, Kirkland and Evans, 1981; Evans and Kirkland, 1988; Javor, 1989) have shown that primary productivity may be remarkably high. Furthermore, studies of sedimentary organic matter have shown that substantial quantities of lipid material may be produced and preserved in these environments. The frequent co-occurrence of sediments rich in organic matter with suitable cap rock lithologies (e.g. sulphates) and potential structure-forming salt bodies make evaporitic environments of particular interest with respect to the formation and preservation of the organic matter, and the generation of hydrocarbon reservoirs. This study considers an evaporitic sequence from the Mulhouse basin (Alsace, France; see Hofmann *et al.*, 1993a for map) which exhibits a rhythmic lithological succession, a feature common to many evaporitic sequences, consisting of alternating marls, anhydrites, halites, and occasional potash (sylvite) horizons. Previous studies on a core section (MAX borehole) from this sequence revealed an evolution in the organic matter contents of the marl horizons (Blanc-Valleron *et al.*, 1991) which exhibited concordance with the evolution of the sedimentary lithofacies. Thus it appears that the factors controlling the sedimentary lithofacies may also be important, directly or indirectly, in determining the organic matter abundance, and hence the hydrocarbon source potential of the marls. The present study aims to investigate the evolution of the sedimentary organic matter in the marls, both in terms of the quantities and "Types" of hydrocarbon constituents through the application of a molecular stratigraphic approach.

GEOLOGICAL SETTING

The Eocene to Miocene sediments of the Upper Rhine Graben, an extensive (300 × 30 km) Tertiary rift system, were deposited in a N to S series of basins related to the post-Variscan and Mesozoic structure (Sittler, 1988). In the south of the Graben the Mulhouse and Sélestat Basins, separated from the Strasbourg and Pechelbronne-Rastatt Basins by the Erstein High, experienced maximum subsidence during the Upper Eocene to the Lower Oligocene. To the north, maximum subsidence occurred later, during the Late Eocene to Middle Oligocene. In the Mulhouse and Sélestat Basins, evaporitic sequences

*Present address: Department of Chemistry, University of York, Heslington, York YO1 5DD, U.K.
†Present address: Netherlands Institute of Sea Research (NIOZ), Division of Marine Biogeochemistry, P.O. Box 59, 1790 AB Den Burg, Texel, The Netherlands.

comprising three (lower, middle and upper) salt formations overlie Middle Eocene clays, limestones and lignites (see Hofmann *et al.*, 1993a for generalised stratigraphic column), interpreted as small lake/bog deposits. The subsidence, and the restriction in connection to the North Sea by the Erstein High south of Strasbourg, allowed for the development of salt layers with potash seams above the lacustrine basal sediments. The upper Salt formation, comprising Salt IV, Salt V and "marls without salt", developed from the Upper Eocene fossiliferous zone, a brackish–marine horizon, through to the Middle Oligocene when marine conditions were re-established as indicated by the presence of foraminiferal marls. At this time the graben linked the North Sea and the Mediterranean through the Hessen Depression. Salt IV, which contains the two thickest potash seams in addition to alternating marls, anhydrites, and halites, has been reported to contain the highest amounts of organic carbon (Blanc-Valleron *et al.*, 1986). The evaporites exhibit concentric zonation about the centre of the *ca* 30 km wide basin, indicating shrinkage of the basin during evaporation, with individual horizons being laterally continuous over large distances, indicating the basin to be fairly shallow.

EXPERIMENTAL

Sampling of F cores for quantitative biomarker analysis

A total of 71 samples (including duplicates; Table 1 and Fig. 1) was selected mainly from two

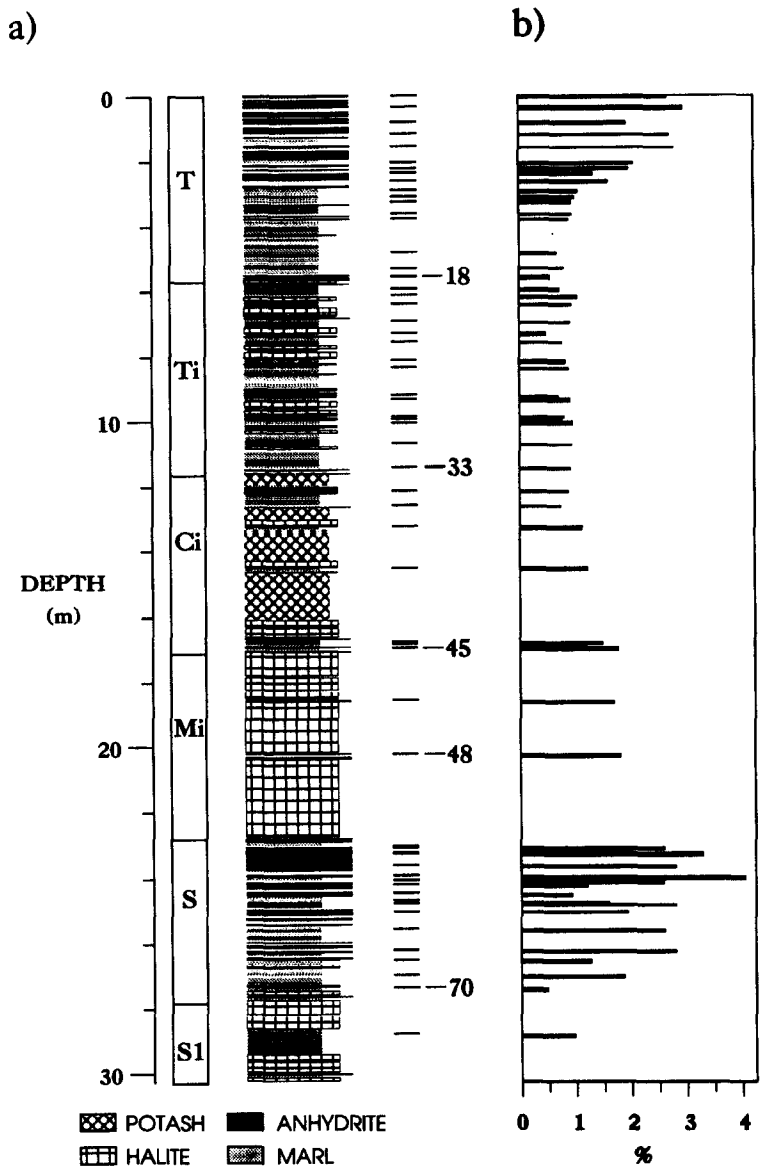

Fig. 1. (a) Detailed lithological column of the cored section (F2 reference core) from the base of the Salt IV unit with sample locations and selected sample numbers indicated. (b) TOC values of the samples collected.

cores (F1 and F3), which cover the stratigraphic section from within the S1 bed (Sd_5) to the base of MS (see Hofmann *et al.*, 1993a). In addition, a number of samples collected from sub-surface exposure in the Amélie Concession (Gallery 830) were included. A number of the marl samples (Table 1)

Table 1. Details of the stratigraphic positions, lithologies, and TOC contents of the samples

Sample number	Bed identification	Depth* (m)	TOC (%)	Lithology
1	T	0.090	2.68	marl
2	T	0.445	2.97	marl
3	T	0.445	2.97	marl
4	T	0.900	1.94	marl
5	T	1.240	2.73	marl
6	T	1.620	2.80	marl
7	T	2.135	2.07	marl
8	T	2.300	1.98	marl
9	T	2.440	1.34	marl + thin anhydrite
10	T	2.690	1.61	marl
11	T	2.995	1.06	marl
12	T	3.165	1.00	marl
13	T	3.335	0.94	marl
14	T	3.685	0.95	marl
15	T	3.830	0.89	marl
16	T	4.870	0.67	marl + thin anhydrite
17	T	5.325	0.80	marl + thin anhydrite
18	T	5.635	0.55	marl + thin anhydrite
19	Ti	5.990	0.72	marl
20	Ti	6.215	1.04	marl
21	Ti	6.440	0.93	marl
22	Ti	6.985	0.92	marl
23	Ti	7.350	0.47	marl
24	Ti	7.600	0.76	marl
25	Ti	8.215	0.83	marl + thin anhydrite
26	Ti	8.415	0.89	marl
27	Ti	9.270	0.70	marl + thin anhydrite
28	Ti	9.385	0.91	marl + thin anhydrite
29	Ti	9.890	0.79	marl
30	Ti	9.970	0.76	marl
31	Ti	10.100	0.95	marl
32	Ti	10.735	0.93	marl
33	Ti	11.485	0.92	marl
34	Ci	12.180	0.87	marl
35	Ci	12.630	0.73	marl
36	Ci	12.630	0.73	marl
37	Ci	12.630	0.73	marl
38	Ci	13.330	1.12	marl
39	Ci	14.565	1.22	marl
40	Ci	14.565	1.22	marl
41	Ci	16.825	1.49	marl
42	Ci	16.825	1.49	marl
43	Ci	16.915	1.19	marl
44	Ci	16.915	1.19	marl
45	Ci	17.015	1.77	marl
46	Ci	17.015	1.77	marl
47	Mi	18.665	1.69	marl
48	Mi	20.315	1.80	marl
49	S	23.110	2.60	marl
50	S	23.135	2.04	marl
51	S	23.275	2.00	marl
52	S	23.315	3.29	marl
53	S	23.650	2.80	marl
54	S	24.010	4.05	marl
55	S	24.140	2.58	marl
56	S	24.250	1.20	marl
57	S	24.540	0.92	marl
58	S	24.805	1.58	marl
59	S	24.825	2.80	marl
60	S	25.065	1.92	marl
61	S	25.065	1.92	marl
62	S	25.630	2.60	marl
63	S	25.630	2.60	marl
64	S	26.275	2.80	marl
65	S	26.275	2.80	marl
66	S	26.275	2.80	marl
67	S	26.275	2.80	marl
68	S	26.595	1.26	marl
69	S	27.060	1.86	marl
70	S	27.460	0.47	marl
71	S1	28.890	0.97	marl

*Depth (in metres) from the top of the T bed (see Fig. 1).

contained very fine anhydrite layers which could not be removed prior to analysis. The presence of the anhydrite does not represent a problem in the organic analysis of the marls since it has been shown that, in the Mulhouse basin, the molecular signal of the organic matter contained in anhydrite facies arises from organic matter associated with very thin layers of marls (Sinninghe Damsté *et al.*, 1993a). Details of the stratigraphic position within the Salt IV formation, lithologies, and total organic carbon contents of the samples are given in Table 1 and in Fig. 1. Total organic carbon (TOC) measurements were obtained by Rock Eval (courtesy of Dr P Hofmann, KFA).

Extraction and fractionation

Prior to extraction, the external surfaces of the marls were cleaned with dichloromethane (DCM) to remove contamination from handling. They were then powdered and Soxhlet-extracted, in the presence of activated copper turnings, for 24h using DCM/Methanol (MeOH) at the azeotropic composition (4:1 v/v). Following extraction, the solvent extract was removed from the copper turnings (blackened in cases where elemental sulphur had been present) and was reduced to a small volume. In a number of cases, further treatment to remove dissolved salts and water was necessary. This was achieved by redissolving the extract in DCM and either washing with water and then separating the two phases, or by adding anhydrous $MgSO_4$ to remove water, followed by centrifugation to remove the $MgSO_4$ and precipitated salts. Internal standards [217 μg/ml n-C_{36} alkane, 136 μg/ml d^4-cholestane labelled at C-2 and C-4, and 41.3 μg/ml 2-methyl-2-(4,8,12-tridecyl)chroman]

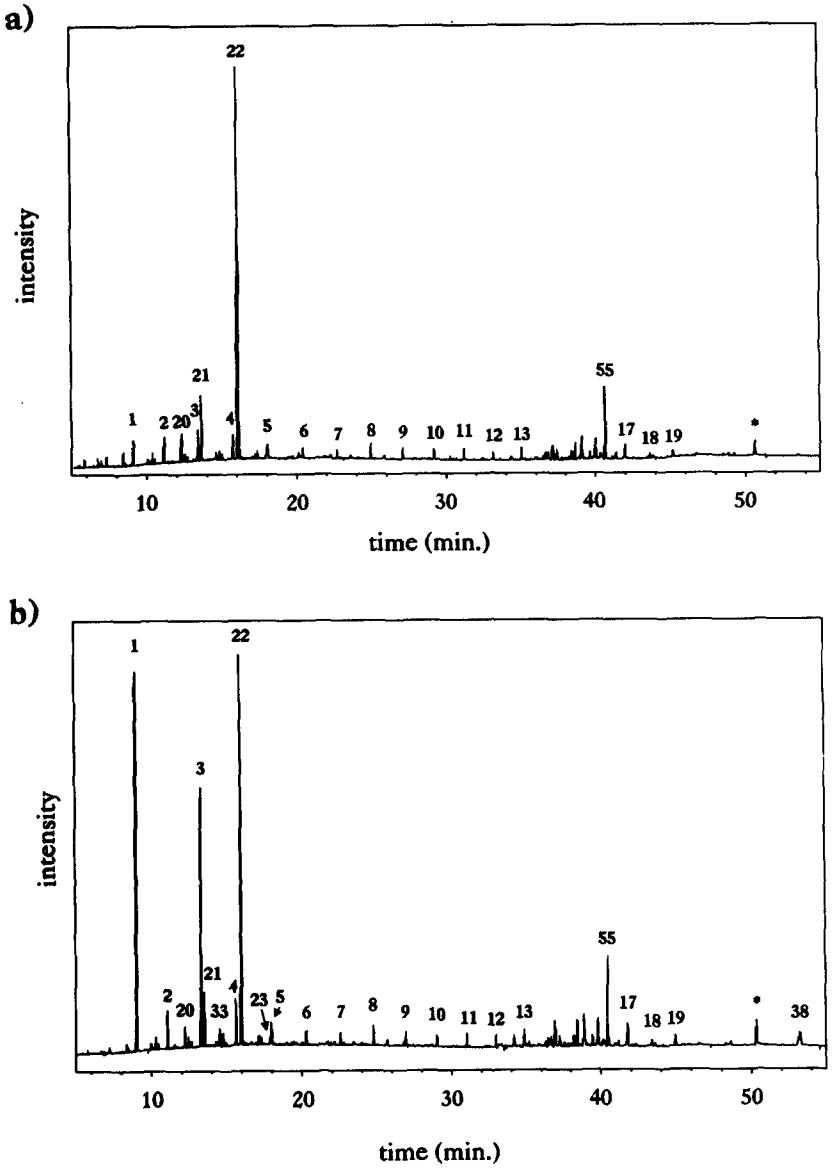

Fig. 2(a) and (b). *Caption on facing page.*

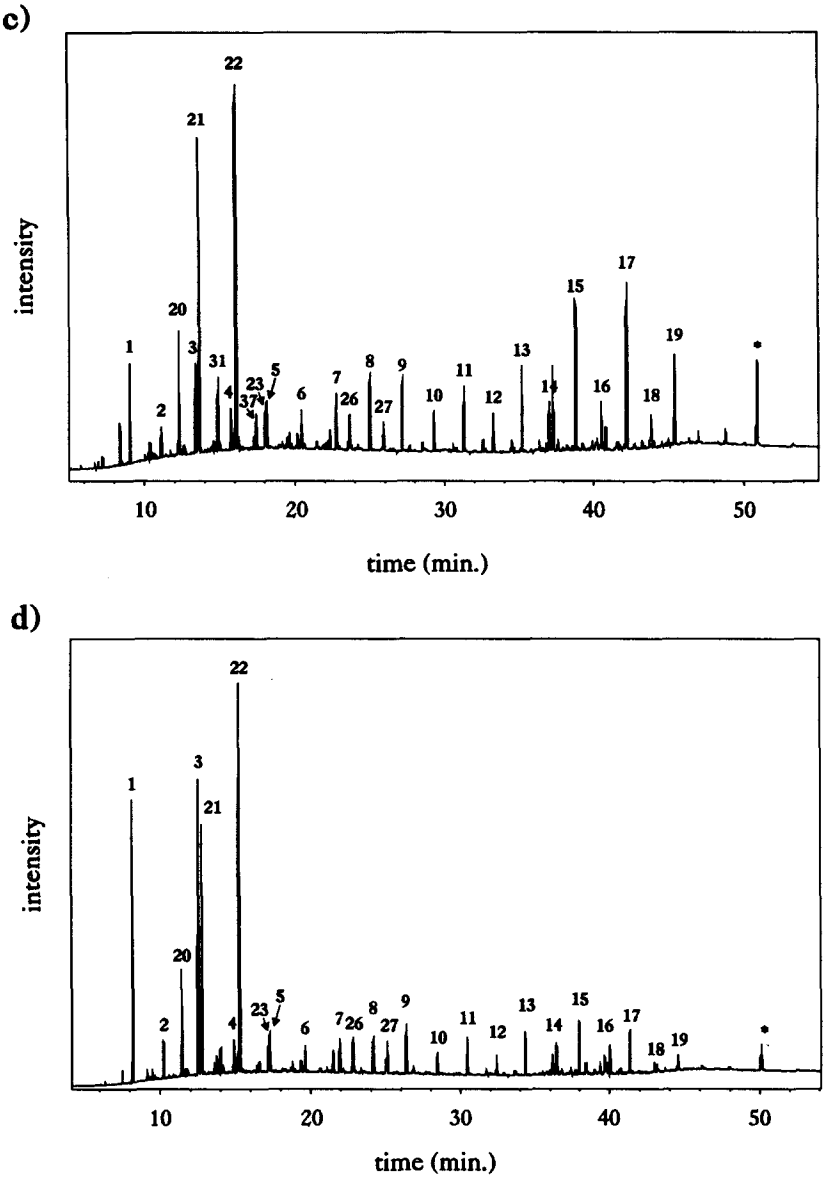

Fig. 2. Gas chromatograms of the aliphatic fractions from (a) sample 1, "Type" A; (b) sample 11, "Type" B; (c) sample 23, "Type" C; (d) sample 17, showing mixed "Type" B/C characteristics. Peak labels correspond to the variable numbers in Table 2 and * to the internal standards.

were added in rough proportion to the amount of total extract (*ca* 100 μl/20 mg), or in constant proportion (10 μl/mg extract) to 10 mg of the extract. Fractionation was carried out using preparative thin layer chromatography (TLC) on pre-cleaned (1:1 DCM:MeOH), activated (150°C for 1 h) silicagel-60 with hexane as developer. The aromatic and aliphatic fractions were recovered from the silica by elution using DCM, or by extraction using hexane and centrifugation, and were reduced to a small volume, transferred to vials and the remaining solvent removed under nitrogen.

Gas chromatography (GC)

GC analyses were carried out either on a Chrompack CP-Sil 5 column (50 m × 0.32 mm i.d., 0.25 μm film) fitted in a Varian 3500 gas chromatograph employing H_2 carrier gas, or on a Carlo Erba 5300 instrument fitted with a similar column with 0.12 μm film thickness employing He as carrier gas. The samples were injected (on column) at 70°C and on the Varian 3500 the injector was programmed to 350°C at 200°C/min. The oven was programmed to 130°C at 20°C/min and then to 320°C at 4°C where it was held for 20 min.

Gas chromatography–mass spectrometry (GC–MS)

GC–MS analyses were performed either on a Finnigan TSQ 70 fitted with a Varian 3140 GC, or on a VG-70s spectrometer connected to a Hewlett Packard 5480 chromatograph. On the TSQ, chromatographic conditions were identical to those used for GC analyses using the Varian 3500. On the VG-70s an identical oven temperature programme was employed using a 25 m column (0.1 μm film thickness) with He as carrier. The TSQ-70 was operated at 70 eV with an emission current of 200 mA over a mass range of 50–650 with a cycle time of 1 s. The VG-70s was operated at 70 eV with a mass range of 40–800 and a cycle time of 1.8 s (resolution 1000). Both full scan acquisition and selected ion monitoring (SIM) were used. GC–MS and GC–MS/MS analyses, used to assign the major 4-Me steranes, were performed on the TSQ 70 employing a DB1701 column (60 m × 0.32 mm i.d., 0.15 μm film; H_2 carrier). The GC oven was programmed from 70°C to 130°C at 20°C/min and then to 320°C at 2°C where it was held for 20 min. GC–MS/MS analyses were performed using Ar as collision gas (0.3 mtorr cell pressure, collision energy −35 V).

Quantification

Quantification of *normal*-, 2-*methyl*(*iso*), 3-*methyl*-(*anteiso*-), isoprenoid (*i*-) alkanes, C_{17} *n*-alkylcyclohexane, and β-carotane was carried out using either VG Minichrom software or a Waters Associates program, by relating GC peak areas to those of the *n*-C_{36} alkane standard. Initial results indicated there were some discrepancies in the quantification, which were related to the solubility of this standard. Accordingly, data were re-processed, and GC peak areas were related to those of the d^4-cholestane. However, it was necessary to make a correction for the amount of cholestane in the samples since it partially co-elutes with the d^4-cholestane. This was achieved by determining the ratio of the intensities of the base peak fragment ions of cholestane (*m*/*z* 217) and d^4-cholestane (*m*/*z* 221), using GC–MS.

Quantification of hopanes, steranes, and methyl steranes, was performed using ICIS software (TSQ-70 data), or VG software (VG-70s) by comparison of peak areas in the *m*/*z* 191, 217, and 231 chromatograms with those in the *m*/*z* 221 chromatograms (equivalent to *m*/*z* 217 of regular steranes), relating to the d^4 cholestane standard. In the case of the hopanes, to allow for the difference in the proportion of the ion current carried by *m*/*z* 191 in comparison with *m*/*z* 217 and 221, a correction factor (1.5) was applied to the hopane data. The correction factor was calculated by comparison of GC and GC–MS peak areas in a sediment hydrocarbon fraction rich in hopanes, with d^4-cholestane added.

Multivariate analysis

Quantitative biomarker data [79 variables, a to ℓ and 1–67, expressed in μg/g organic carbon (C org.); Table 2] for the 71 samples were processed using the SYSTAT statistical analysis programme (SYSTAT Inc.). The resultant data matrices for the loadings of the variables and object scores were transferred to Quattro spreadsheets (Borland International) for data display.

RESULTS AND DISCUSSION

Studies of the TOC contents of a number of samples obtained from a core (MAX borehole) covering the Salt IV formation showed the major part of the organic carbon to be associated with the marl horizons, and the presence of at least two levels of maximum TOC within the marls of the Salt IV formation (Blanc-Valleron *et al.*, 1991). TOC maxima were located at the top of the S bed and T bed, respectively above and below the potash horizon within Ci [cf. Fig. 1(a)]. Accordingly, in the present study, samples from two cores (F1 and F3), which cover the base of the Salt IV formation from within S1 to the top of T, were selected to cover the whole extent of the TOC profile over more than one "cycle". The location of the samples (Table 1) is indicated in Fig. 1(a). The TOC measurements obtained herein [Table 1, Fig. 1(b)] show a similar profile to that observed previously and demonstrate a sufficiently high sampling frequency to characterise the profile. The samples which exhibit high TOC contents tend to be quite waxy, with very fine laminae consisting of alternating clastic and organic-rich layers. In contrast, the samples with very low TOC contents are lighter in colour and exhibit a more obvious varved appearance. A number of the low TOC samples contain sandy horizons and exhibit cross-bedding, indicative of a generally higher energy depositional environment than that during deposition of the high TOC samples. On the basis of TOC contents, atomic ratios (H/C and O/C) and alkane GC distributions, three families or "Types" of organic matter were defined previously (Blanc-Valleron *et al.*, 1991). Thus, "Types" A (high TOC) and B (intermediate TOC) were suggested to mainly algal and "Type" C (low TOC) mainly terrestrial and bacterial in origin. Differences were apparent in the GC distributions (Blanc-Valleron *et al.*, 1991). Thus, "Type" A samples typically showed [cf. Fig. 2(a) and Table 2] a bimodal *n*-alkane distribution maximising at *n*-C_{16-18} and at *n*-C_{22} or *n*-C_{24} and exhibiting slight even predominance, and a high relative abundance of phytane with pristane/phytane (Pr/Ph) ratios <0.3. Samples of "Type" B typically showed [cf. Fig. 2(b) and Table 2] high relative abundances of *n*-C_{15} and *n*-C_{17}, with a second lower maximum exhibiting an odd predominance and centred around *n*-C_{29}, Pr/Ph typically $\leqslant 0.3$, and low abundance of *i*-C_{21} to *i*-C_{25} alkanes. The "Type" C samples [cf. Fig. 2(c) and Table 2] were dominated by the odd chain length *n*-alkanes maximising around C_{29}, high (>0.5) Pr/Ph ratios, prominent *i*-C_{21} to *i*-C_{25} alkanes and greater

Table 2. Variables used in the multivariate analysis

Variable number*	Variable
1	*n*-pentadecane
2	*n*-hexadecane
3	*n*-heptadecane
4	*n*-octadecane
5	*n*-nonadecane
6	*n*-eicosane
7	*n*-heneicosane
8	*n*-docosane
9	*n*-tricosane
10	*n*-tetracosane
11	*n*-pentacosane
12	*n*-hexacosane
13	*n*-heptacosane
14	*n*-octacosane
15	*n*-nonacosane
16	*n*-triacontane
17	*n*-hentriacontane
18	*n*-dotriacontane
19	*n*-tritriacontane
20	2,6,10-trimethylpentadecane (*nor*-pristane)
21	2,6,10,14-tetramethylpentadecane (pristane)
22	2,6,10,14-tetramethylhexadecane (phytane)
23	2,6,10,14-tetramethylheptadecane
24	2,6,10,14-tetramethyloctadecane
25	2,6,10,14-tetramethylnonadecane
26	2,6,10,14,18-pentamethylnonadecane
27	2,6,10,14,18-pentamethyleicosane
28	2,6,10,15,19,23-hexamethyltetracosane
29	2-methylpentadecane
30	2-methylhexadecane
31	2-methylheptadecane
32	2-methyloctadecane
33	undecylcyclohexane
34	3-methylpentadecane
35	3-methylhexadecane
36	3-methylheptadecane
37	3-methloctadecane
38	β-carotane
39	2,8-dimethyl-2-(4,8,12-trimethyltridecyl)chroman
40	2,7,8-trimethyl-2-(4,8,12-trimethyltridecyl)chroman
41	2,5,7,8-tetramethyl-2-(4,8,12-trimethyltridecyl)chroman
a	C_{27} hopane
42	17α(H),21β(H)-25-norhopane
43	17β(H),21α(H)-25-norhopane
44	17α(H),21β(H)-hopane
45	17β(H),21α(H)-hopane
46	17α(H),21β(H)-22*S*-homohopane
b	gammacerane
47	17α(H),21β(H)-22*R*-homohopane
48	17α(H),21β(H)-22*S*-bishomohopane
49	17α(H),21β(H)-22*R*-bishomohopane
c	17α(H),21β(H)-22*S*-trishomohopane
d	17α(H),21β(H)-22*R*-trishomohopane
e	17α(H),21β(H)-22*S*-tetrakishomohopane
f	17α(H),21β(H)-22*R*-tetrakishomohopane
g	17α(H),21β(H)-22*S*-pentakishomohopane
h	17α(H),21β(H)-22*R*-pentakishomohopane
i	20*S* 5α(H),14α(H),17α(H)-cholestane
50	20*R* 5α(H),14α(H),17α(H)-cholestane
j	20*S* 5α(H),14α(H),17α(H)-methylcholestane
51	20*R* 5β(H),14α(H),17α(H)-methylcholestane
52	20*R* 5α(H),14α(H),17α(H)-methylcholestane
53	20*S* 5α(H),14α(H),17α(H)-ethylcholestane
54	20*R* 5β(H),14α(H),17α(H)-ethylcholestane
55	20*R* 5α(H),14α(H),17α(H)-ethylcholestane
56	C_{28} ring A methyl sterane
57	C_{28} ring A methyl sterane
58	C_{29} ring A methyl sterane
59	C_{29} ring A methyl sterane
60	20*R*-4α-methyl-5α(H),14α(H),17α(H)-24-methylcholestane
61	20*R*-4β-methyl-5α(H),14α(H),17α(H)-24-methylcholestane
62	C_{30} ring A methyl sterane
63	20*R*-4α-23,24-trimethylcholestane
k	20*R*-4α-23,24-trimethylcholestane
l	C_{30} ring A methyl sterane
64	20*R*-4α-23,24-trimethylcholestane
65	20*R*-4α-23,24-trimethylcholestane
66	20*R*-4β-23,24-trimethylcholestane
67	20*R*-4β-23,24-trimethylcholestane

*All variables were used in the covariance matrix, numbered variables relate to those used in the correlation matrix.

relative abundances of *iso*-and *anteiso*-alkanes in the range C_{16}–C_{19}. In the present study, the alkane profiles of a larger number of samples have been examined. These reveal distributions which do not clearly fall into the three families (cf. Blanc-Valleron *et al.*, 1991). For example, the distribution in Fig. 2(d) shows high relative abundances of *n*-C_{15} and *n*-C_{17} ("Type" B) but high Pr/Ph and high relative abundances of *i*-C_{21} to *i*-C_{25} ("Type" C). Likewise, there are other samples which would be difficult to assign as "Type" A or B distributions on the basis of the alkane profiles.

Two different sterane profiles have been reported previously (Betts *et al.*, 1991). In one case, corresponding to "Type" B or "Type" C alkane distributions, the steranes were dominated by the C_{29} $\alpha\alpha\alpha$ 20*R* component [cf. Fig. 3(a)]. In the second case, corresponding to "Type" A alkane distributions, approximately equal relative abundances of the C_{27} and C_{29} $\alpha\alpha\alpha$ 20*R* components were apparent, along with additional contributions of ring A methylated steranes, particularly 4-Me components. Again, however, the present study shows a wider range of distributions, particularly in relation to the relative abundances of C_{27} and C_{29} steranes [e.g. Fig. 3(b)]. Indeed, a range of relative abundances of C_{27} and C_{29} $\alpha\alpha\alpha$ 20*R* components is apparent in samples which would be considered as "Type" A, based on the simple classification of alkane distributions outlined above.

The 4-Me sterane distributions of a number of the samples have been examined in greater detail by GC–MS using a medium polarity stationary phase. Almost complete resolution of the 4,23,24-trimethylcholestane and 4-methyl-24-ethylcholestane components was achieved within both the 4α and 4β series [Fig. 4(b) and Table 2]. Components were assigned using MS–MS monitoring of the *m/z* 414–98 transition [Fig. 4(a); cf. Thomas *et al.*, 1993]. The proportion of the *m/z* 98 ion in the dinosterane isomers is much greater than in their 24-Et counterparts due to the more favourable loss in the side-chain through a rearrangement process. In all of the samples examined in this way the abundance of the summed dinosterane isomers considerably outweighs that of the 24-Et components. Despite recent reports of minor amounts of dinosterol (the presumed precursor) in an aquatic plant (Klink *et al.*, 1992) and a marine diatom (Volkman *et al.*, 1993), in accordance with previous studies (Boon *et al.*, 1979; de Leeuw *et al.*, 1983; Robinson *et al.*, 1984; Summons *et al.*, 1987, 1993) we consider the most likely source of dinosterane in such high abundance relative to the 4-desmethyl steranes to be marine dinoflagellates. Hence, the presence of dinosterane as a dominant component of the 4-Me steranes in a limited number of samples suggests a significant marine contribution to the sedimentary organic matter (cf. Goodwin *et al.*, 1988; Summons *et al.*, 1987). Notably, marine foraminifera have also been identified in a number of

the marl samples from this sequence (Hofmann, 1992).

Hopanes are present in low relative abundance in all of the samples, and their distributions are relatively constant within the sample suite. Slight differences are apparent, with the "Type" A samples sometimes exhibiting only slightly higher relative abundances of the $>C_{33}$ components [e.g. Fig. 3(c)]. Within the aromatic fractions significant differences are apparent in the chroman distributions; the variations in the distributions have been attributed to changes in the salinity of the upper part of the water column during deposition of the marls in the sequence (Sinninghe Damsté *et al.*, 1993b).

In summary, the impression from the alkane GC profiles and the sterane profiles obtained by GC–MS is that these profiles do not fall clearly into three discrete "Types" or families: rather, over the 59 individual samples, the differences become blurred and, apart from the 4-Me steranes, relate mainly to differences in the relative abundances of the same components. In order to investigate further the differences in distribution over the sequence, a quantitative investigation was carried out.

Quantitative molecular description of marls

The abundances of individual components were determined relative to the organic carbon contents of

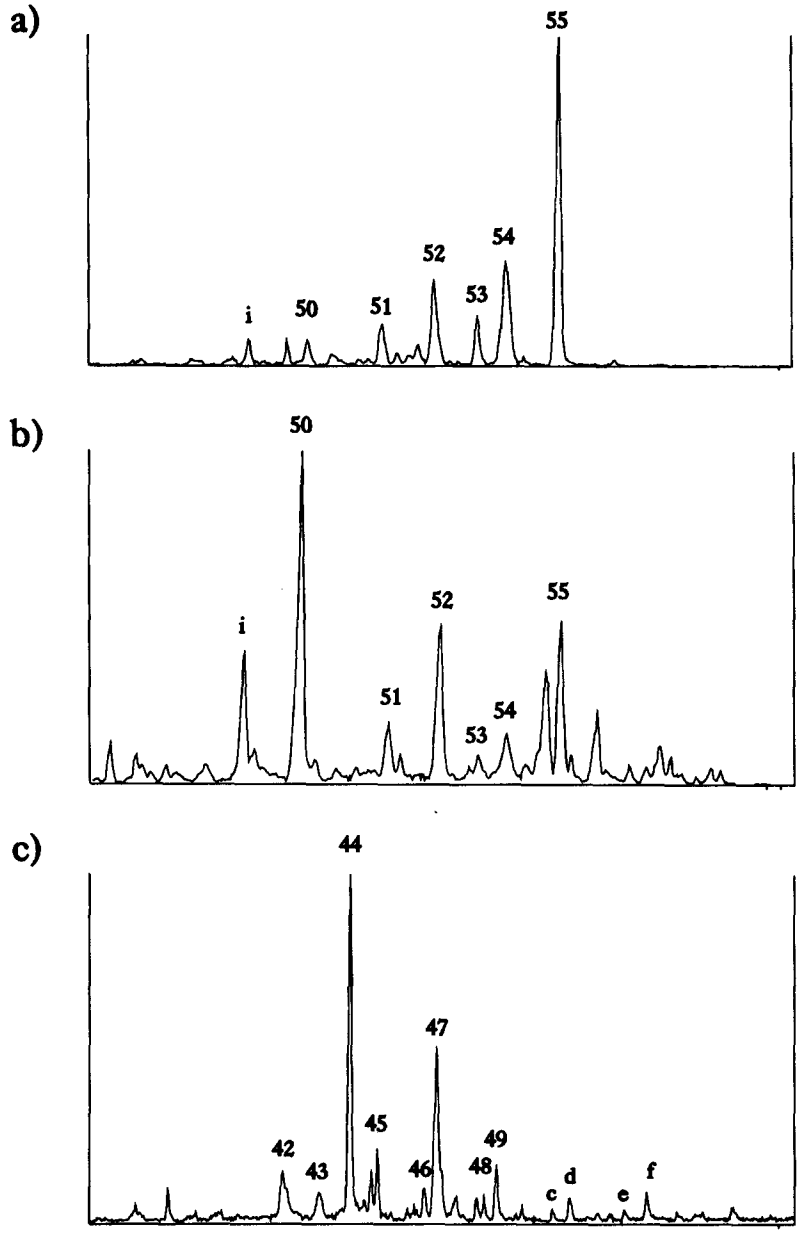

Fig. 3. Mass chromatograms showing characteristics profiles of (a) desmethyl steranes (m/z 217) of "Type" B/C samples; (b) desmethyl steranes (m/z 217) of "Type" A samples; and (c) hopanes (m/z 191) of "Type" A samples. Peak labels correspond to the variable numbers in Table 2.

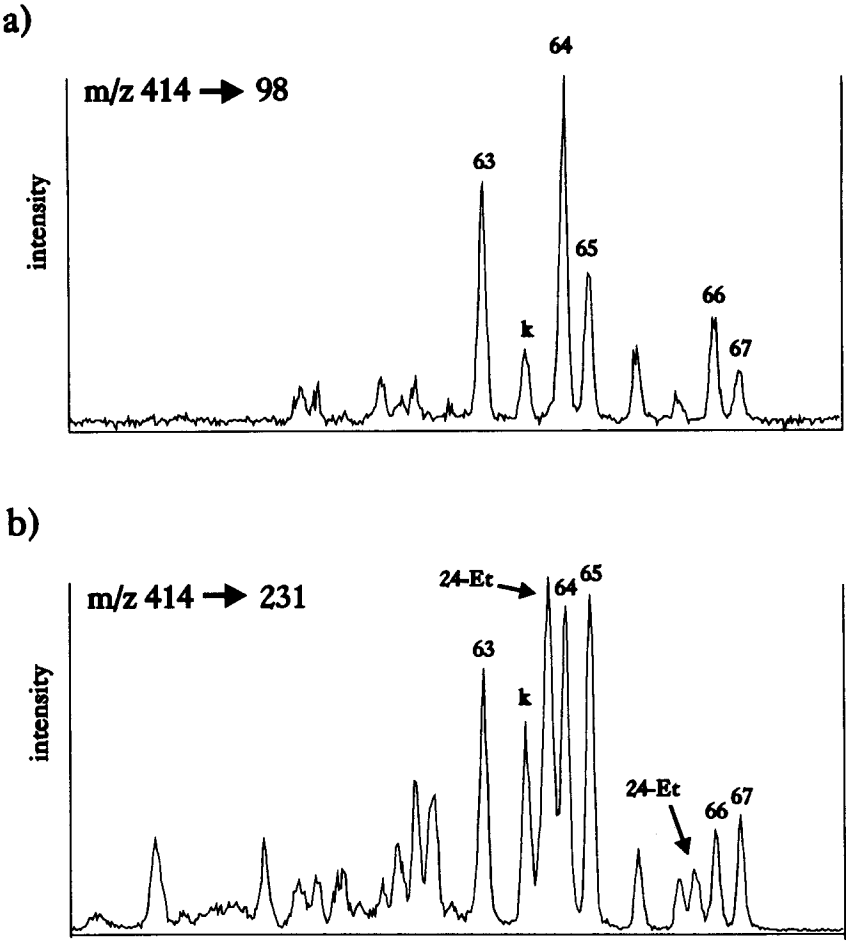

Fig. 4. Mass chromatograms from GC–MS/MS analysis, showing profiles of the ring A-methylated steranes in sample 53 ("Type" A). (a) Transition m/z 414–98 (dinosterane and isomers); and (b) m/z 414–231 (C_{30} ring A methyl steranes). Peak labels correspond to the numbers in Table 2.

the samples. To avoid losses of the more volatile alkanes (i.e. n-C_{15-17}) extracts were only blown down with N_2 for the minimum time to remove solvent. In addition, the reproducibility between duplicate samples was good.

Principal components analysis (PCA)

PCA was used to allow comparison of the samples based on the quantities of the biological markers listed in Table 2. Analysis of the raw data set, without normalisation or standardisation, shows that the outer variance (variance between samples) is significantly greater than the inner variance [variance between duplicates; Fig. 5(a)]. The first two principal components [PC1 and PC2; Fig. 5(a)], accounting for 63% of the variance, do not separate the samples into discrete classes as might perhaps have been expected from the previous classification into three "Types", A, B, and C, as described above. Examination of the loadings of variables on PC1, which accounts for 49% of the total variance [Fig. 5(b)] shows that the concentration of phytane (variable 22) dominates this component. The PCA technique discriminates samples on the basis of the direction and amplitude to which the distributions of their variables deviate from that of the average (the zero-point spectrum). Accordingly, the two extreme distributions on PC1 correspond to samples having high amounts (positive scores) and low amounts (negative scores) of phytane relative to the zero-point spectrum. Similarly, PC2 [14%; Fig. 5(c)] is dominated by the n-C_{15} and n-C_{17} alkanes, the only significant variables on this component. In this case the two extreme distributions simply relate to samples having low amounts (positive scoring) and high amounts (negative scoring) respectively, of n-C_{15} and n-C_{17}.

The major variations in the hydrocarbon compositions over the sequence are described by the first two PCs, these representing the most important compositional changes in terms of the concentrations of components. To some extent this relates to the classification made by examining the relative abundances of components from inspection of the GC and GC–MS traces, but suggests perhaps that there

are not discrete types of distribution. The main point arising from the PC analysis is the variation in the amount of phytane; in essence, the two extremes in positive and negative scores on PC1 can be considered as end members, with their distributions relating to "Types" A and C respectively. Clearly, high amounts of n-C_{15} and n-C_{17} do not relate to a separate "Type" B distribution (see above) since samples with both positive and negative scores on PC1 (relating to both "Types" A and C) have high

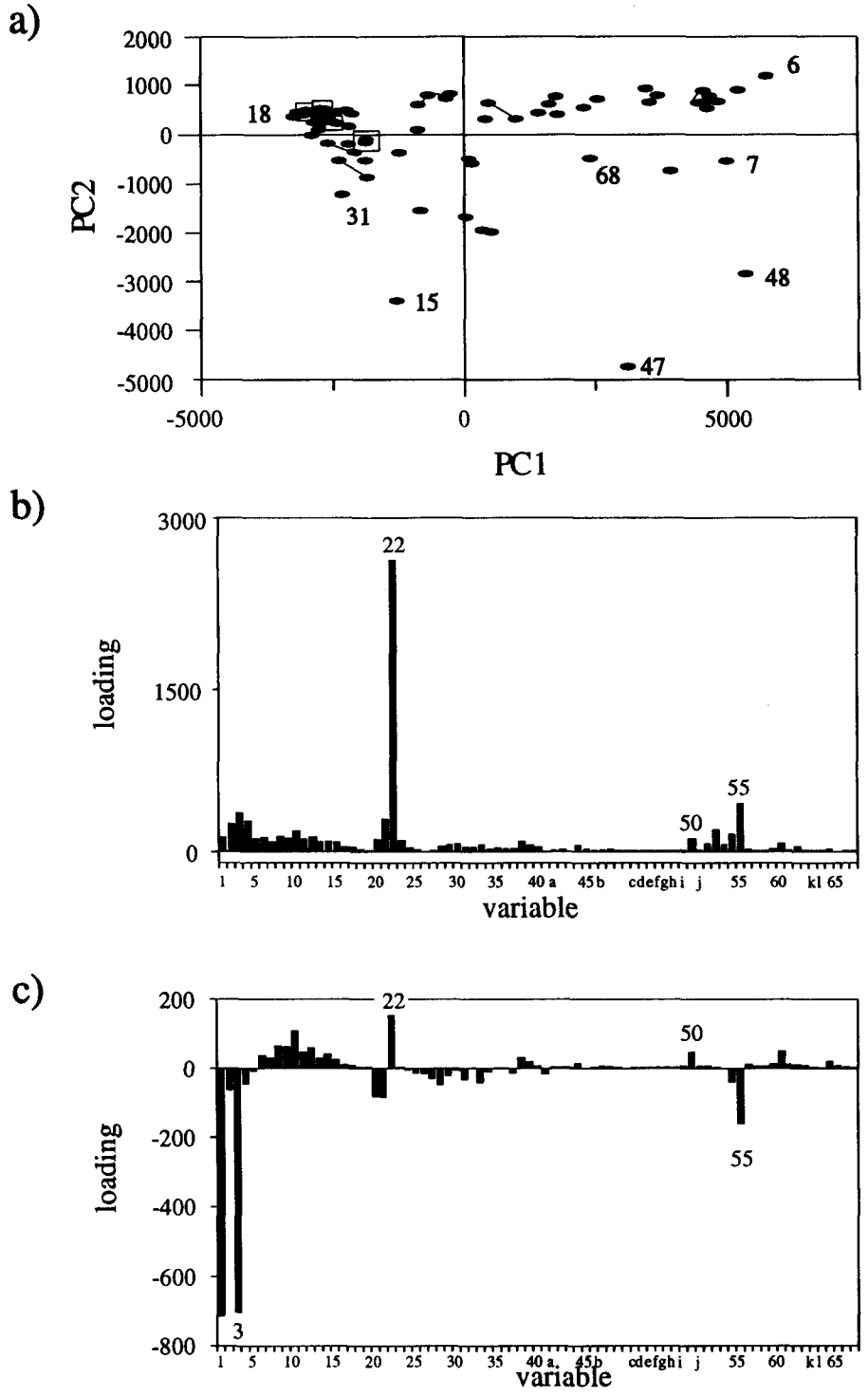

Fig. 5. (a) Scores plot of the first two PCs of the covariance matrix (points representing duplicates are either linked or are enclosed by boxes); (b) loadings plot of the variables on PC1; (c) loadings of the variables on PC2. For identification of variables, see Table 2.

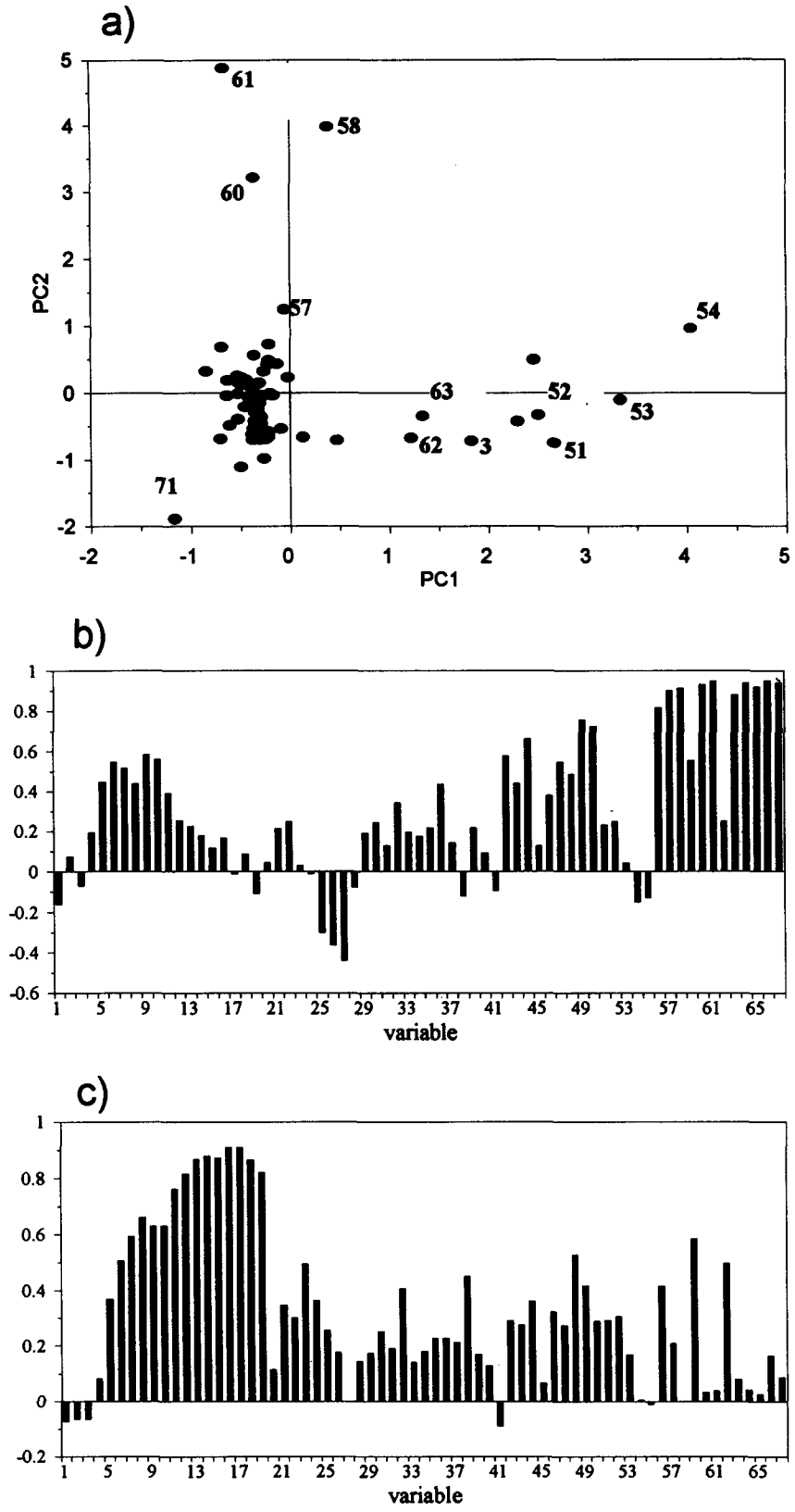

Fig. 6. (a) Scores plot of the first two PCs of the correlation matrix; (b) loadings plot of the variables on PC1; (c) loadings of the variables on PC2. For identification of variables, see Table 2.

amounts (negative scores) of these components. The variation in the amount of phytane could be the result of contributions from different sources, or of changes in the productivity and/or preservation during the deposition of the sediments (see below). Since the variations in the amounts of the C_{15} and C_{17} *n*-alkanes do not correlate with the variations in the amounts of phytane, it is apparent that these

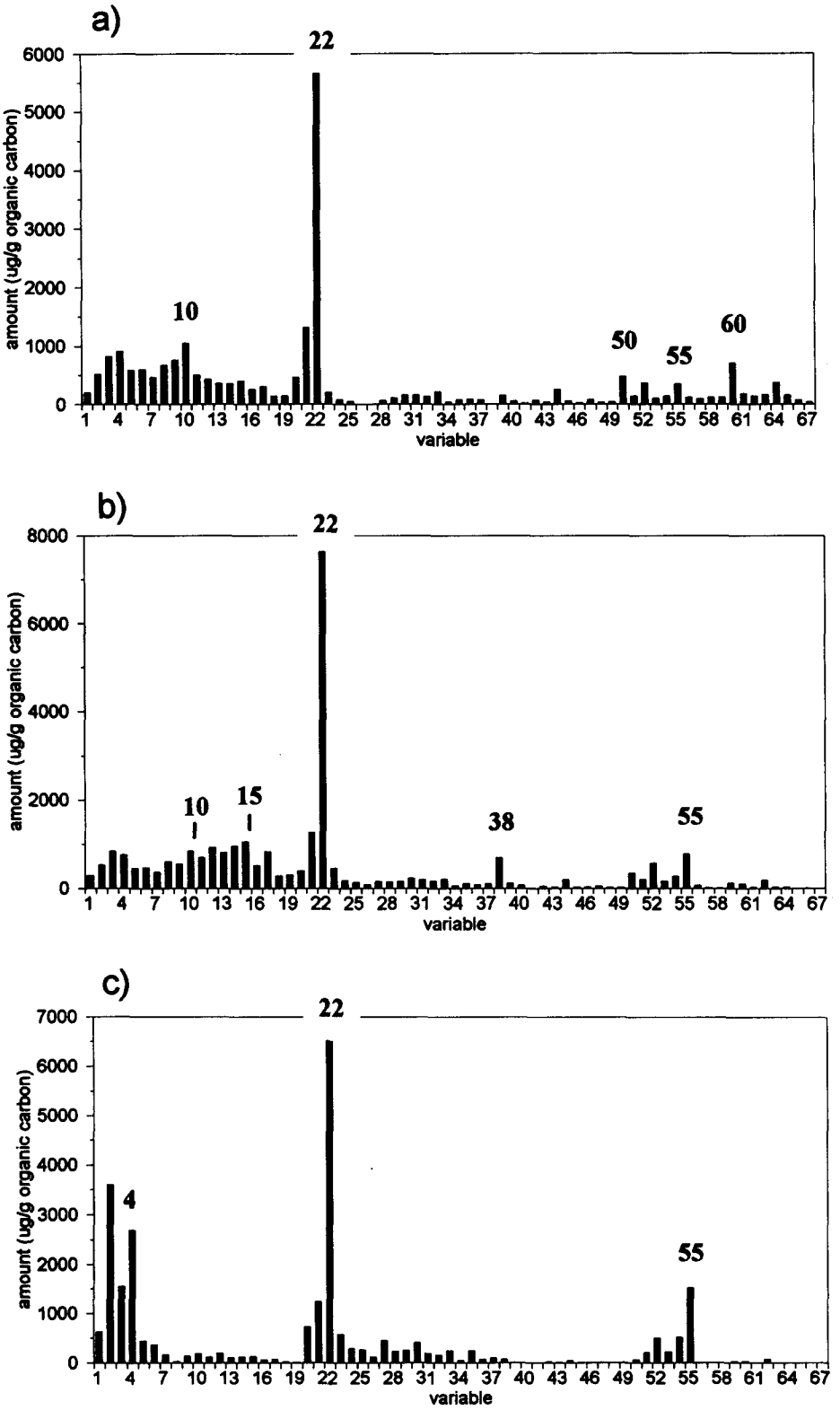

Fig. 7(a)–(c). *Caption on facing page.*

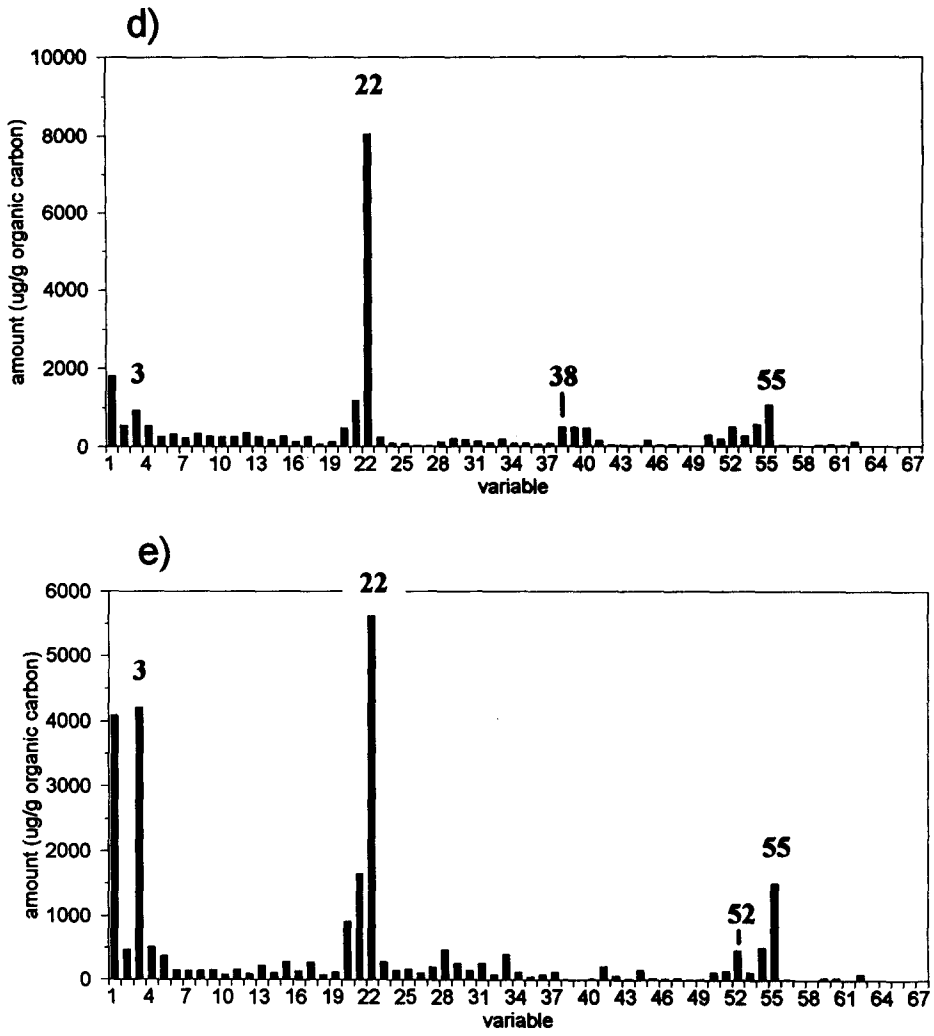

Fig. 7. Distributions of variables in highest scoring samples on (a) PC1 (sample 54); (b) PC2 (sample 61); (c) PC3 (sample 71); (d) PC4 (sample 7); (e) PC5 (sample 47). For identification of variables, see Table 2.

n-alkane components represent a contribution mainly from a distinct source and thus their abundances may reflect changes in the conditions within the depositional environment.

Variations exemplified by PC3, PC4 etc. are considered unimportant because of their low percentage of explained variance, the significance of which is questionable. This largely relates to the problem of scaling of the data. Because there are large differences in the variances in the variables, much of the total variance in the data set is associated with the variance in the variables themselves. Thus, components with high variance (e.g. phytane) will dominate the analysis and may mask covariances of interest. Furthermore, because of these inequalities, correlations may be either difficult to identify, or even be meaningless. Hence, in order to avoid overemphasis of the variables with high variance and therefore allow examination of subtle variations and correlations within the data set, it is necessary to remove the effect of variable scale. Accordingly, the data were autoscaled (standardised by the mean and standard deviation; Kowalski and Bender, 1972) to give the resultant correlation matrix. The initial processing of the correlation matrix indicated that a number of variables (those with consistently low abundances; or sometimes exhibiting partial coelutions on GC; a to *ℓ* in Table 2) should be excluded from the analysis, as they were apparent over numerous PCs. After exclusion of variables a to *ℓ*, extraction of the first five PCs explained 81% of the total variance in the data. Examination of the loadings of variables on the resulting PCs 1–5 revealed only a limited amount of geochemically interpretable information. Following VARIMAX rotation of the data, however, geochemically significant information was obtained. A scores plot of the first two components [Fig. 6(a)] supports the interpretation above, i.e. that the hydrocarbon distributions do not simply represent members of discrete classes A, B, and C. Rather, consideration of

the concentrations of a wide variety of components, including steranes, indicates that the distributions are better described as intermediates between end members. The non-discrete nature of the range of scores on PC1 suggests that the changes giving rise to the distributional differences in the hydrocarbons were not catastrophic, but rather tended to be gradual and resulted from gradual changes in depositional conditions. The communalities of the variables (Table 3) show that for many of them a very high proportion of their variance is accounted for by extraction of five PCs. PC1 (rotated components explain 15% of the variance) is dominated by all but two of the ring A methyl steranes (variables 56–67, excluding 59 and 62), with a significant contribution to the PC from $\alpha\alpha\alpha$ C_{27} 20*R* sterane [cholestane, variable 50; Fig. 6(b), Table 3]. Because of the association of cholestane (50) and dinosterane isomers (63–67) with this PC [Fig. 6(b), Table 3], it appears to represent a marine algal contribution, implying a marine source for the majority of the ring A methyl steranes. Interestingly, the C_{30} and the C_{32} 22*R* $\alpha\beta$ hopanes (44,49) show a high association with this PC, suggesting that in this sequence their abundance may also be related to a marine (bacterial) contribution. In addition to significant contributions of methyl steranes, the sample which scores highest on PC1 [sample 54; Fig. 7(a)] shows high abundances of regular steranes, phytane and *n*-alkanes in the range C_{16}–C_{25}, with a slight even predominance due to the minor maxima at *n*-C_{18} and *n*-C_{24}. PC2 (12% variance) is dominated by the *n*-alkanes $>C_{22}$ [Fig. 6(c), Table 3] with lesser contributions from other variables. The distinction of these *n*-alkanes (especially variables 11–19) from the lower carbon number species (especially 1–4) clearly indicates at least two sources of *n*-alkanes [Fig. 6(c)]. Notably, both the even and odd carbon number *n*-alkanes $>C_{22}$ contribute about equally to this PC. This indicates that variations in the odd/even predominance are of relatively low significance and that variations in the concentrations of these components are important in discriminating the distributions. The sample which scores highest on PC2, having the highest concentrations of *n*-alkanes [sample 61; Fig. 7(b)], exhibits an odd/even predominance only above *n*-C_{29} and has abundant *n*-alkanes from *n*-C_{22} to *n*-C_{28} with slight even/odd predominance (presumably also contributing to components $>n$-C_{28}). This contrasts with samples having a strong odd/even predominance of higher *n*-alkanes [cf. Fig. 2(c)] and which contain lower concentrations of such components. Hence, there are at least two contributions to the *n*-alkanes $>C_{22}$, including one of higher plant origin (odd/even predominance) and one, possibly of algal origin (even/odd predominance). PC3 (10%, Table 3) is dominated by *n*-C_{16}, *n*-C_{18}, *i*-C_{21}, *i*-C_{22} the C_{17} and C_{19} *iso*alkanes and the C_{17} *anteiso*alkane. It appears, therefore, to be associated with contributions from bacterial sources though these remain unidentified. Interestingly, the highest scoring distribution [sample 71; Fig. 7(c)] also contains high abundances of regular steranes and phytane.

PC4 (9%) is dominated by phytane, the mono- and di-methyl chromans, the C_{29} and C_{30} $\beta\alpha$ hopanes, and the C_{28} and C_{29} regular steranes (Table 3). Hence, sample 7 [Fig. 7(d)], which scores highest on this PC, contains one of the highest concentrations of phytane and regular steranes. The contribution of the mono- and di-methyl chromans suggests that this PC relates to conditions of elevated salinity in the surface waters (Sinninghe Damsté *et al.*, 1993b). The high contributions to PC4 from phytane and the C_{28} and C_{29} steranes, which are of algal origin, is noteworthy. Phytane in sediments may be derived principally from two sources, either the phytol side chain of chlorophyll (Volkman and Maxwell, 1986), or the lipids of archaebacteria (Risatti *et al.*, 1984; ten Haven *et al.*, 1987). The association of phytane and the C_{28} and C_{29} steranes with PC4 indicates that the phytane in the marls is derived mainly from algal sources. This point is further discussed below. PC5 (8%) is dominated by the C_{15} and C_{17} *n*-alkanes, *nor*-pristane, pristane, squalane, C_{18} *iso*alkane, C_{17} alkylcyclohexane, and C_{19} *anteiso*alkane (Table 3). The association of the C_{15} and C_{17} *n*-alkanes on PC5 suggests that this PC in part describes a cyanobacterial contribution since these components or likely precursors (alkenes and acids) have been identified as significant extractable components of cyanobacteria (Han and Calvin, 1964; Han *et al.*, 1968a, b; Winters *et al.*, 1969; Boudou *et al.*, 1986; Grimalt *et al.*, 1992) or as products released from pyrolysis of resistant biopolymeric material isolated from a cyanobacterium (Chalansonnet *et al.*, 1988). The sample scoring highest on PC5 (sample 47) is shown in Fig. 7(e).

In summary, the PC analysis shows that the hydrocarbon distributions of the samples are not best represented as three discrete families of "Types" (A, B, and C). Rather, they are better described as intermediates between end members approximating to "Types" A and C. After autoscaling and rotation, the major differences among the samples are revealed, which can be attributed to changes in the relative contributions from different source organisms and variation in the extent of marine influence.

Molecular stratigraphy

The principal components analysis provides the basis for examination of the samples in a stratigraphic context. A number of the features apparent from PCA can be attributed to changes during deposition of the sequence, in the (i) productivity and/or preservation; (ii) contributions from different algal sources; (iii) contributions from different bacterial sources.

The original classification of samples into the "Types" A, B, and C was explained by assuming that differences in the nature of the organic inputs were apparent. Thus, "Type" A and B samples

Table 3. Communalities (%) of the variables on the five principal components of the correlation matrix and variance explained by the PCs

	Communalities*					
Variable	PC1	PC2	PC3	PC4	PC5	Cumulative
1	−3	−1	−1	1	62	68
2	1	0	61	1	8	71
3	0	0	4	2	59	66
4	4	1	69	3	9	85
5	20	14	37	3	14	87
6	30	26	32	7	1	95
7	27	35	21	8	1	92
8	19	44	11	6	0	80
9	34	40	13	3	0	90
10	31	40	16	2	0	90
11	15	58	14	5	0	93
12	6	67	17	4	0	94
13	5	75	7	5	1	94
14	3	77	10	2	0	92
15	1	76	1	3	2	84
16	3	83	5	0	2	93
17	0	83	0	1	4	88
18	1	75	0	2	4	81
19	−1	67	−7	0	4	80
20	0	1	16	1	63	81
21	4	12	16	3	41	76
22	6	9	23	48	6	92
23	0	24	54	4	8	91
24	0	13	61	1	17	92
25	−9	6	36	0	30	81
26	−13	3	0	−19	26	61
27	−19	0	16	−10	22	67
28	−1	2	9	5	47	62
29	4	3	23	14	36	80
30	6	6	55	8	13	89
31	2	4	24	0	56	85
32	12	17	42	9	9	88
33	4	2	12	9	55	82
34	3	3	5	8	51	71
35	5	5	55	5	11	82
36	19	5	19	4	23	70
37	2	4	22	2	44	74
38	−1	20	2	35	−2	61
39	5	3	0	52	1	61
40	1	2	0	45	3	50
41	−1	−1	−8	20	32	62
42	33	8	14	8	4	68
43	19	8	3	48	3	82
44	44	13	20	4	1	81
45	2	0	−2	61	2	67
46	14	10	4	31	7	67
47	30	7	2	37	2	79
48	23	28	2	18	2	73
49	57	17	14	1	0	90
50	52	8	5	27	0	93
51	5	9	26	48	2	90
52	6	9	25	42	3	86
53	0	3	12	56	1	72
54	−2	0	9	59	7	77
55	−2	0	13	53	10	77
56	66	17	6	4	0	94
57	81	4	1	0	0	87
58	83	0	0	0	0	84
59	31	34	20	4	0	89
60	87	0	1	3	0	90
61	90	0	0	2	0	92
62	6	25	23	31	0	86
63	77	1	0	0	0	78
64	88	0	0	0	0	89
65	85	0	0	0	0	85
66	91	3	0	0	0	94
67	89	1	0	0	0	90
Variance explained						
Rotated components	15	12	10	9	8	54
Total	22	18	15	14	12	81

*Negative sign indicates negative loading of the variable on a PC.

were considered to be mainly of algal origin, with "Type" B and C samples containing a greater relative contribution of terrestrially-derived organic matter (Blanc-Valleron *et al.*, 1991; Betts *et al.*, 1991), and a greater relative abundance of higher molecular weight *n*-alkanes with odd carbon numbers of presumed higher plant origin (e.g. Eglinton *et al.*, 1962).

The depth concentration profile of the sum of all steranes [Fig. 8(a)] reflects changes in the algal contribution recorded over the sequence. The profile shows a similarity to the TOC profile [Fig. 1(b)], and to the phytane [Fig. 8(b)], with maxima and minima recorded in the same stratigraphic horizons. The correlation between the total steranes and phytane and the high abundances of these components (summed steranes up to 5000 μg/g C org., phytane up to *ca* 9000 μg/g C org.) points to the phytane being derived mainly from algal sources, as ascribed from the PC analysis. Similarly, the concentrations of all of the individual major regular steranes exhibit a similar profile to those of phytane and the TOC (see below). Hence, it appears likely that the profile results from changes in either the algal productivity, and/or in the preservation potential over the sequence. Hofmann *et al.* (1993b) have estimated that, over the interval examined, the production of "aquatic organic matter" (algal and bacterial) was greatest towards the tops of the S and T beds, and lowest in the Ti bed, essentially following the TOC profile. Of the components investigated herein on a quantitative basis, the distributions of those (e.g. phytane and steranes) derived from the primary producers reflect most strongly the TOC profile. Furthermore, the proportion of labile to non-extractable organic matter is much greater in the higher TOC samples than in the low TOC samples. In this context, it is noteworthy that the distributions of alkanes released from asphaltenes, polar fractions and kerogens of samples derived from anoxic and often evaporitic palaeoenvironments, through the selective cleavage of S–S and C–S bonds, are generally dominated by phytane and steranes (Sinninghe Damsté *et al.*, 1988, 1990; de Leeuw and Sinninghe Damsté, 1990; Kohnen *et al.*, 1991a, b; Adam *et al.*, 1992; Hofmann *et al.*, 1992; Koopmans *et al.*, 1993). We suggest, therefore, that in the high TOC samples the increase in phytane and steranes as a proportion of C_{org} results mainly from incorporation of functionalised lipids into macromolecular fractions via sulphide linkages and subsequent release (early generation), following low temperature cleavage of the sulphur bonds. Indeed, although the amounts of organic sulphur in the kerogens are low, it has been shown that marls from the stratigraphic horizons where the TOC is highest (towards the tops of the S and T beds) contain the highest amounts of organic sulphur, suggesting that sulphur quenching occurred to a greater extent during deposition of these parts of the sequence (Sinninghe Damsté *et al.*, 1993c). Furthermore, Koopmans *et al.* (1993) have demonstrated that

sulphur-rich geomacromolecules are degraded at low temperatures and that phytane, steranes, and elemental sulphur are important products. In the present study, elemental sulphur (detected by blackening of activated copper during extraction) was present in samples with higher TOC contents, and absent from samples from the TI bed and the base of the T bed. Also, Sinninghe Damsté *et al.* (1993c) have shown that, in comparison with other immature samples from evaporite settings, extracts of the Mulhouse Basin marls are surprisingly low in organic sulphur components. This provides further circumstantial evidence that sulphur quenching of algal lipids followed by early generation, accounts, at least in part, for the increase in the quantities of labile organic matter in the marls and for the changes in the relative abundances of a number of the lipids over the sequence.

The pristane/phytane ratio is shown in Fig. 8(c). Although the explanation given by Didyk *et al.* (1978) for the operation of the ratio as an indicator of water column redox potential is probably oversimplified,

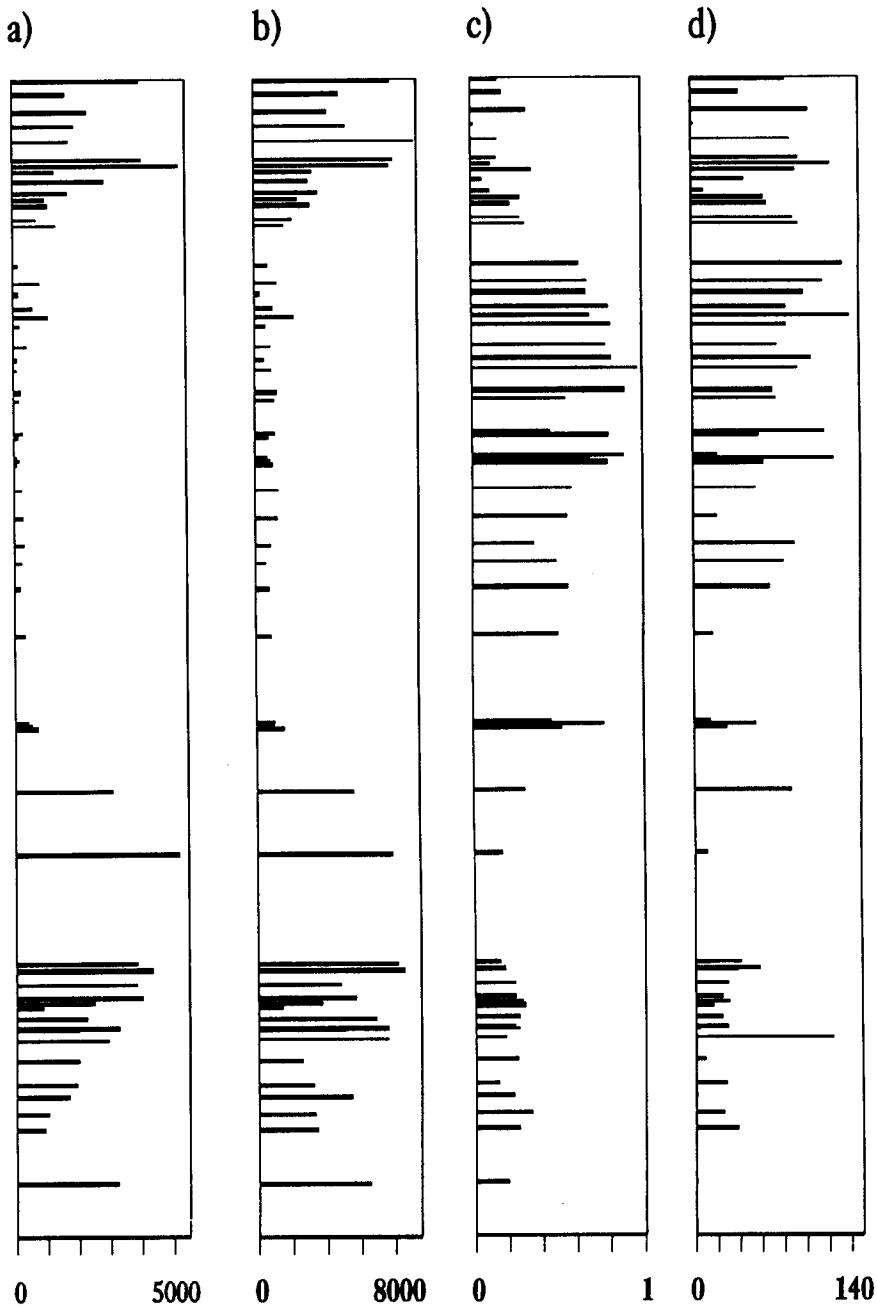

Fig. 8. Depth profiles of (a) summed concentrations of desmethyl and ring A-methylated steranes; (b) concentration of phytane; (c) pristane/phytane ratio; (d) concentration of *n*-alkanes $(C_{31} - C_{30} + C_{33} - C_{32})/2$.

the evidence does indirectly point to an empirical relationship, given a predominantly algal source for the phytane. The lowest Pr/Ph ratios [Fig. 8(c)] are associated with the samples which have the highest TOC values, and the highest concentrations of algal derived components (see above). Conversely, the highest ratios correspond to samples with the lowest TOC values and highest abundances of terrestrially derived organic matter (Hofmann *et al.*, 1993b). The variation in the ratio results mainly from variations in the concentration of phytane. the abundance of pristane remains relatively constant throughout the sequence. It seems likely, therefore, that reduction in the extent of oxygenation resulted from increases in algal productivity and the production of H_2S by sulphate reduction, as indicated by the sulphur quantities (see above). Indeed, in two of the higher TOC samples where the alkyl porphyrin distributions have been examined, there is evidence for the operation of an active sulphur cycle and for photic zone anoxia, from the presence of porphyrins derived from green photosynthetic bacteria (Keely and Maxwell, 1993).

From PCA on the correlation matrix, it was concluded that there are at least two contributions to the *n*-alkanes $> C_{22}$ and that the most important changes in concentration relate to a contribution other than that from higher plants (odd/even predominance in the range C_{27}–C_{33}). In an attempt to reveal the differences in the higher plant contribution, Fig. 8(d) shows a depth plot of the concentration to which the odd carbon number *n*-alkanes exceed the even carbon numbers in the range C_{29}–C_{32}. From the plot, the highest contributions tend to be associated with samples from Mi through to T [cf. Fig. 1(a)]. This is in broad agreement with the conclusion of Hofmann *et al.* (1993b) that the contribution of continental-derived organic matter increased during the middle section of the sequence (particularly within the Ti bed and lower part of the T bed). The plot in Fig. 8(d) indicates, however, that the higher plant contribution to the hydrocarbons is low, whereas Hofmann *et al.* (1993b) concluded that the terrestrial contribution, where high, represents a significant proportion of the total organic matter. This relates to differences in the two approaches, one based on the abundances of alkanes, the other on visual (microscopic) estimation of the quantities of terrestrial organic matter. The former approach will only take into account terrestrial organic matter contributions which yield extractable organic matter, whereas the latter approach will consider the bulk of terrestrially derived material, including reworked and refractory material.

The PCA above indicated contributions from different algal sources to the samples, as revealed by the correlation of the C_{27} regular steranes and certain ring A methyl steranes, including dinosteranes, and by the correlation of the C_{28} and C_{29} regular steranes with β-carotane and phytane. The depth profiles of the total regular steranes [Fig. 9(a)], dinosterane isomers [Fig. 9(b)], cholestane [variable 50; Fig. 9(c)] show that the last two components maximise around the TOC maxima [Fig. 1(b)] but at depths slightly above the maximum in the regular steranes, indicating changes in the algal contribution. This is clearer [Fig. 9(d)] in a plot of the C_{27}/C_{29} sterane ratio (variable 50 over 55) which is similar to the depth profile of the summed dinosterane isomers [Fig. 9(b)]. Since the dinosteranes and cholestane are ascribed a marine origin (see above), variations in the marine influence are apparent, being most obvious at the tops of the S and T beds [cf. Fig. 1(a)]. This influence is associated with changes in the regular sterane distributions, from a dominance of C_{29} components to the less frequent dominance of C_{27} components. Lacustrine settings are frequently dominated by organisms which produce mainly C_{29} sterols [cf. Volkman, 1986), although certain marine algae also produce predominantly C_{29} sterols (Volkman *et al.*, 1993). We suggest, therefore, that the changes in the sterane distributions reflect marine ingressions into a lacustrine environment, introducing nutrients and leading to increases in the algal productivity. Further evidence for marine influences comes from the occurrence of tests of benthic marine foraminifera throughout the sequence (Hofmann, 1992). In addition, microscopic examination of a number of samples very closely related (stratigraphically) to those investigated in this study indicate the abundances of foram tests to be greater in the samples from around the TOC maximum in the T bed (Keely and Hofmann, unpublished observation). It appears, therefore, that the depositional setting of the marls was predominantly lacustrine but with variable contributions of marine waters.

The PC analysis indicated a further source input by way of the abundances of the C_{15} and C_{17} *n*-alkanes [Fig. 10(a)]. These components, attributed to cyanobacterial sources (see above), maximise just prior to the main increase in the regular steranes [Fig. 9(a)], suggesting that the organisms thrived when the marine influence was lower.

Variations in bacterial sources are not as clear as for the algal sources. The components *i*-C_{21} and *i*-C_{22} are mainly associated with PC3, suggesting similar source organisms. In contrast, *i*-C_{23} is associated with both PCs 3 and 5, *i*-C_{24} with PCs 1, 4, and 5, and *i*-C_{25} with PCs 1, 3, 4, and 5 (Table 3), suggesting multiple sources, or differences in the diagenetic fates of the precursor lipids. Although the origins of the C_{21}–C_{24} components are uncertain, the C_{25} isoprenoid alkanes are generally assumed to be related to the ether lipids of archaebacteria, for example methanogens (Risatti *et al.*, 1984) and halophilic bacteria [cf. Waples *et al.*, 1974). Depth plots show a great deal of similarity in the concentrations of the components [e.g. *i*-C_{22} and *i*-C_{25}; Fig. 10(b) and (c) respectively], indicating them all to be derived from bacterial sources. The only appreciable difference is that with increasing carbon

number from i-C_{21} to i-C_{25} the abundance maximum shifts from the S bed to the T bed, most likely reflecting differences in the bacterial sources between the two horizons. However, on the whole, the C_{21}–C_{25} isoprenoids do not show a marked variation in abundance over the sequence.

The abundance of all hopanes [Fig. 10(d)] show, like the steranes, similarities to the TOC profile [Fig. 1(b)], although these similarities are not as pronounced as for the steranes. As for the steranes, the individual components exhibit different depth profiles. Thus, the C_{29} and C_{30} components [e.g. C_{30} $\beta\alpha$, variable 45; Fig. 11(a)] exhibit different profiles to the $\alpha\beta$ C_{31} 22R and $\alpha\beta$ C_{33} 22R [e.g. C_{33} $\alpha\beta$, variable c; Fig. 11(b)] components. These differences probably also reflect changes in the bacterial populations during the deposition of the sequence.

CONCLUSIONS

Consideration of the alkane distributions and the concentrations of a number of the components in these distributions, and the application of PCA, reveals gradual changes in the organic matter preserved in the marls over the TOC cycle at the base of the Salt IV formation. The results indicate a

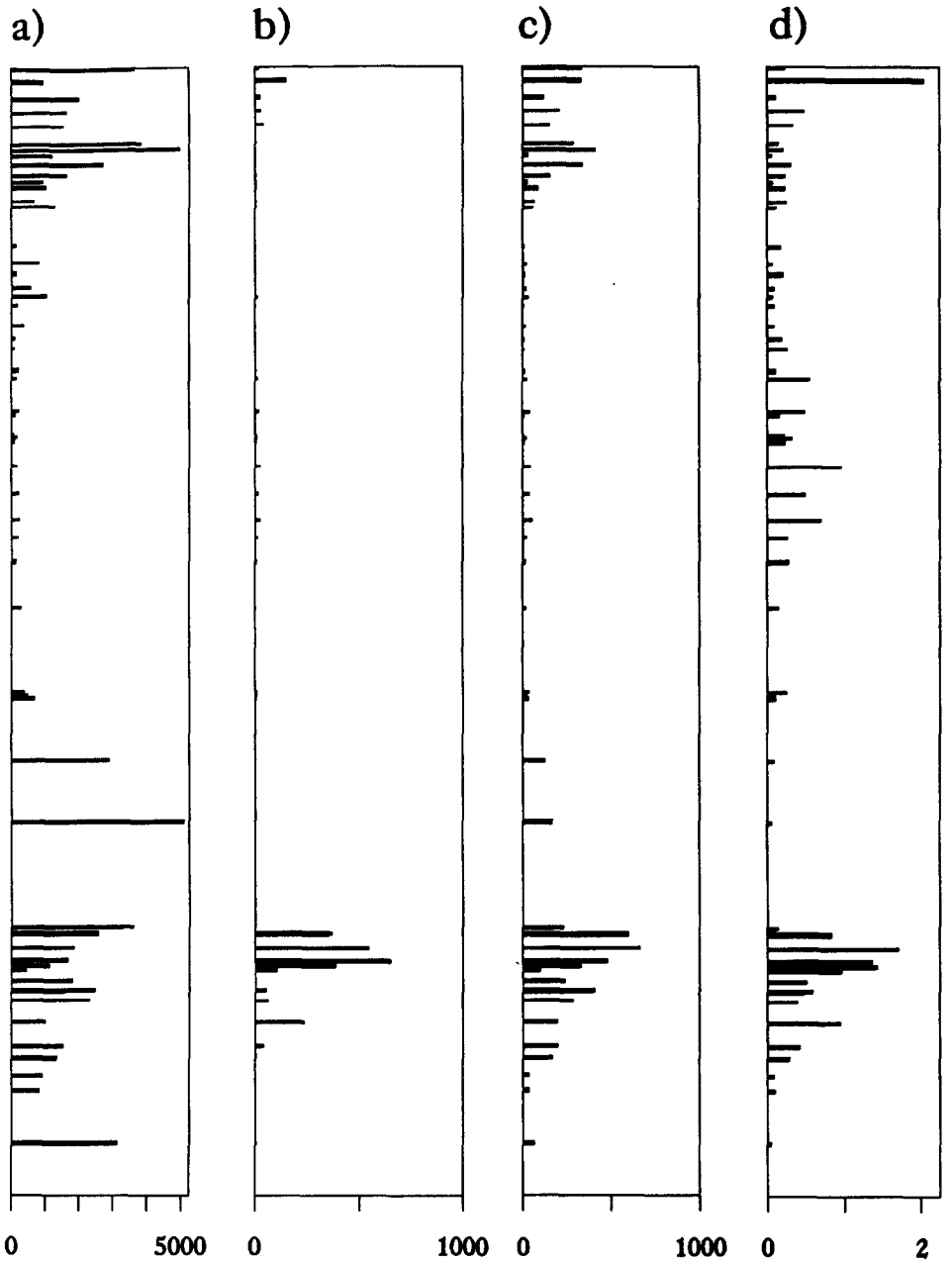

Fig. 9. Depth concentration profiles of (a) sum of desmethyl steranes; (b) sum of dinosterane isomers; (c) cholestane; (d) ratio of the C_{27}/C_{29} $\alpha\alpha\alpha$ 20R steranes.

high degree of variability in the concentrations and the distributions and the frequency with which the changes may occur. Thus, the presence of two main end member distributions is apparent. These end members can be considered as approximating to "Type" A and C distributions described previously, on the basis of alkane relative abundances. These appear to relate to a lacustrine setting with low algal productivity and/or preservation ("Type" C), with increasing algal productivity and preservation resulting from an increased contribution of marine waters, leading to the "Type" A end member hydrocarbon distribution. Hence, major increases in the concentrations of algal-derived components indicate increased productivity with a consequent depletion in oxygenation, generation of anoxic conditions which even extended into the photic zone and which led to greater preservation of organic matter. During periods when anoxic conditions prevailed, it is suggested that interaction between precursor lipids and inorganic sulphur species resulted in incorporation of sulphur linked species. Low temperature cleavage of the S–S and C–S bonds then generated higher concentrations of predominantly phytane and

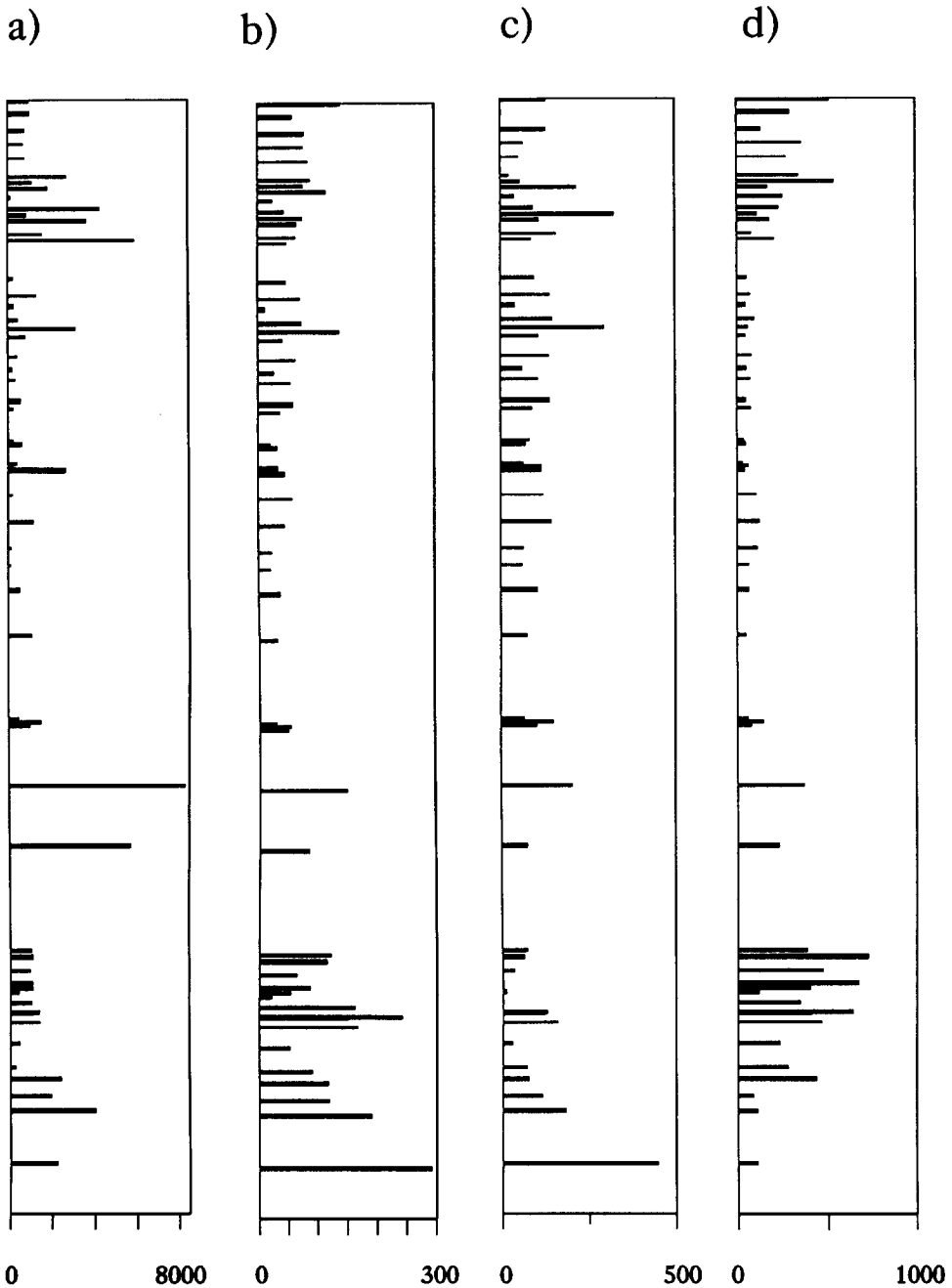

Fig. 10. Depth profiles of the concentrations of (a) sum of C_{15} and C_{17} *n*-alkanes; (b) C_{22} isoprenoid; (c) C_{25} isoprenoid; (d) sum of hopanes.

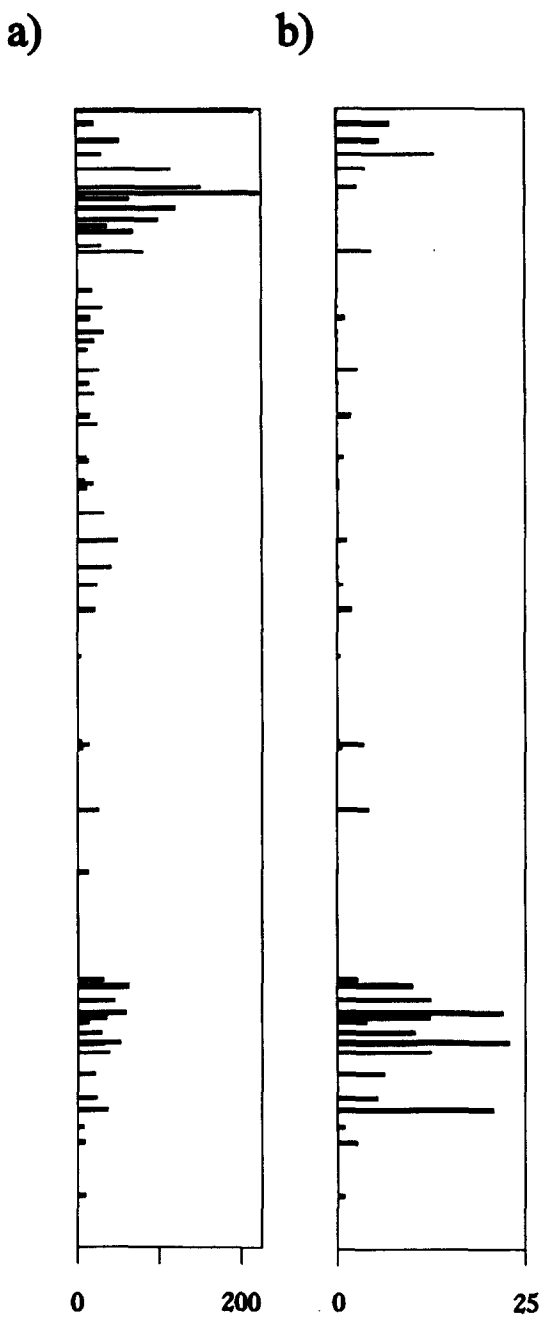

Fig. 11. Depth concentration profiles of (a) C_{30} $\beta\alpha$ hopane; (b) C_{33} $\alpha\beta$ 22*R* hopane.

steranes and resulted in higher proportions of labile organic matter associated with the marls deposited during these periods.

During the deposition of the marls, systematic changes in the primary producer community occurred, as revealed by differences in the depth plots of the concentrations of a number of algal-derived components. These changes appear to have been influenced by the extent of the connection to the sea. The generation of the quantities of salt deposits in the basin suggests some form of connection between a fairly shallow basin and the sea. In general, the lowest amounts of organic matter are found in the sediments which are intercalated with halite and thin anhydrites (S1 and Ti beds, Fig. 1). The hydrocarbon profiles from these sediments relate to the "Type" C end member distribution, consistent with a relatively greater terrestrial contribution and accounting for higher relative abundances of higher plant-derived *n*-alkanes. The evidence of a marine contribution is most apparent in marls from both the S and T beds, which immediately overlie S1 and Ti, where the halite horizons are notably thinner and are absent from the upper regions of the beds. In contrast to the halite horizons, the anhydrites become thicker and more frequent. The increased thickness of the anhydrites further supports the suggestion of a greater marine influence, hence supply of sulphates, in the upper parts of the S and T beds.

Acknowledgements—This work was performed under the auspices of the ENOG (European Network of Organic Geochemistry laboratories) and has benefited from scientific discussion within the group. ENOG comprises Laboratoire de Géochimie, IFP, Rueil-Malmaison, France; Institute of Petroleum and Organic Geochemistry, KFA, Jülich, Germany; Laboratoire de Chimie Organique des Substances Naturelles, Université Louis Pasteur, Strasbourg, France; Organic Geochemistry Unit, Delft University of Technology, The Netherlands; Organic Geochemistry Unit, University of Bristol, U.K., and receives funding from the European Economic Community [EEC contract N SCI-0021-C(TT)]. We thank Dr P Hofmann for TOC measurements, and the NERC for HPLC and mass spectrometric facilities (GR3/6619) and for a Research Fellowship to BJK (GR3/7731). This is NIOZ contribution number 306.

REFERENCES

Adam P., Mycke B., Schmidt J. C., Connan J. and Albrecht P. (1992) Steroid moieties attached to macromolecular petroleum fraction via di- or polysulfide bridges. *Energy Fuels* **6**, 553–559.

Betts S. E., Sinninghe Damsté J. S., de Leeuw J. W. and Hofmann P. (1991) Facies determination in a Tertiary evaporitic sequence (Mulhouse Basin, France) with an emphasis on the assessment of palaeosalinity: a molecular geochemical approach. In *Organic Geochemistry. Advances and Applications in Energy and the Natural Environment* (Edited by Manning D.), pp. 343–345. Manchester Univ. Press.

Blanc-Valleron M.-M. (1986) Enseignments géoligiques tirés de l'étude systématique de la matière organique d'un bassin salifère. Le bassin potassique de Mulhouse (Alsace, France). *C.R. Acad. Sci. Paris* **302, Serie II,** 825–830.

Blanc-Valleron M.-M., Gely J.-P., Schuler M., Dany F. and Ansart M. (1991) Organic matter associated with evaporites of the lower part of Salt IV (Lower Oligocene) in the Mulhouse Basin (Alsace, France). *Bull. Soc. geol. France* **162,** 113–122.

Boon J. J., Rijpstra W. I. C., de Lange F., de Leeuw J. W., Yoshioka M. and Shimizu Y. (1979) Black Sea sterol—a molecular fossil for dinoflagellate blooms. *Nature (London)* **277,** 125–127.

Boudou J. P., Trichet J., Robinson N. and Brassell S. C. (1986) Lipid composition of a Recent Polynesian microbial mat sequence. *Org. Geochem.* **10,** 705–709.

Chalansonnet S., Largeau C., Casadevell E., Berkaloff C., Peniguel G. and Couderc R. (1988) Cyanobacterial resistant biopolymers. Geochemical implications of the

properties of *Schizothrix* sp. resistant material. *Org. Geochem.* **13,** 1003–1010.

Didyk B. M., Simoneit B. R. T., Brassell S. C. and Eglinton G. (1978) Organic geochemical indicators of palaeoenvironmental conditions of sedimentation. *Nature* **272,** 216–222.

Eglinton G., Hamilton R. J., Raphael R. A. and Gonzalez A. G. (1962) Hydrocarbon consituents of the wax coatings of plant leaves: a taxonomic survey. *Nature* **193,** 739–742.

Evans R. and Kirkland D. W. (1988) Evaporitic environments as a petroleum source. In *Evaporites and Hydrocarbons* (Edited by Schreiber B. C.), pp. 256–299. Columbia Univ. Press, New York.

Goodwin N. S., Mann A. L. and Patience R. L. (1988) Structure and significance of C_{30} 4-methyl steranes in lacustrine shales and oils. *Org. Geochem.* **19,** 509–530.

Grimalt J. O., de Wit R., Teixidor P. and Albaiges J. (1992) Lipid biogeochemistry of *Phormidium* and *Microcoleus* mats. *Org. Geochem.* **19,** 509–530.

Han J. and Calvin M. (1964) Hydrocarbon distributions of algae and bacteria, and microbiological activity in sediments. *Proc. Natl. Acad. Sci. U.S.A.* **64,** 436–443.

Han J., McCarthy E. D., Calvin M. and Benn M. H. (1968a) Hydrocarbon constituents of the blue-green algae *Nostoc muscorum, Anacystis nidulans, Phormidium luridum* and *Chlorogloea frischii. J. Chem. Soc.* (*C*), 2785–2791.

Han J., McCarthy E. D., van Hoeven W., Calvin M. and Bradley W. H. (1968b) Organic geochemical studies—II. A preliminary report on the distribution of aliphatic hydrocarbons in algae, in bacteria, and in a recent lake sediment. *Proc. Natl. Acad. Sci. U.S.A.* **59,** 29–37.

ten Haven H. L., de Leeuw J. W., Rullkötter J. and Sinninghe Damsté J. S. (1987) Restricted utility of the pristane/phytane ratio as a palaeoenvironmental indicator. *Nature* **330,** 641–643.

Hofmann P. M. (1992) *Sedimentary Facies, Organic Facies, and Hydrocarbon Generation in Evaporite Sediments of the Mulhouse Basin, France.* Berichte des Forschungszentrums Jülich No. 2664.

Hofmann I. C., Hutchison J., Robson J. N., Chicarelli M. I. and Maxwell J. R. (1992) Evidence for sulphide links in a crude oil asphaltene and kerogens from reductive cleavage by lithium in ethylamine. *Org. Geochem.* **19,** 371–387.

Hofmann P. M., Huc A. Y., Carpentier B., Schaeffer P., Albrecht P., Keely B. J., Maxwell J. R., Sinninghe Damsté J. S., de Leeuw J. W. and Leythaeuser D. (1993a) Organic matter of the Mulhouse Basin, France: a synthesis. *Org. Geochem.* **20,** 1105–1123.

Hofmann P. M., Leythauser D. and Carpentier B. (1993b) Palaeoclimate controlled accumulation of organic matter in Oligocene evaporite sediments of the Mulhouse Basin. *Org. Geochem.* **20,** 1125–1138.

Javor B. (1989) *Hypersaline Environments: Microbiology and Biogeochemistry.* Springer, Berlin.

Keely B. J. and Maxwell J. R. (1993) The Mulhouse Basin: evidence from porphyrin distributions for water column anoxia during deposition of marls. *Org. Geochem.* **20,** 1217–1225

Kirkland D. W. and Evans R. (1981) Source-rock potential of evaporitic environment. *Am. Assoc. Petrol. Geol. Bull.* **65,** 181–190.

Klink G., Dreier F., Buchs A. and Gulacar F. O. (1992) A new source for 4-methyl sterols in freshwater sediments: *Ultricaria neglecta* L. (Lentibulariacaceae). *Org. Geochem.* **18,** 757–763.

Kohnen M. E. L., Sinninghe Damsté J. S. and de Leeuw J. W. (1991a) Biases from natural sulphurisation in palaeoenvironmental reconstruction based on hydrocarbon biomarker distributions. *Nature* (*London*) **349,** 775–778.

Kohnen M. E. L., Sinninghe Damsté J. S., Kock-van Dalen A. C. and de Leeuw J. W. (1991b) Di- or polysulfide-bound biomarkers in sulphur-rich geomacromolecules as revealed by selective chemolysis. *Geochim. Cosmochim. Acta* **55,** 1375–1394.

Koopmans M., Lewan M. D., Sinninghe Damsté J. S. and de Leeuw J. W. (1993) Maturity-related changes in abundance and composition of organic sulphur compounds and sulphur-containing geomacromolecules studied by hydrous pyrolysis. In *Organic Geochemistry Poster Seminar from the 16th International Meeting on Organic Geochemistry, Stavanger 1993* (Edited by Øygard K.), pp. 125–128.

Kowalski B. R. and Bender C. F. (1972) Pattern recognition. A powerful approach to interpreting chemical data. *J. Am. Chem. Soc.* **94,** 5632–5639.

de Leeuw J. W., Rijpstra W. I. C., Schenck P. A. and Volkman J. E. (1983) Free, esterified and residual bound sterols in Black Sea Unit I sediments. *Geochim. Cosmochim. Acta* **47,** 455–465.

de Leeuw J. W. and Sinninghe Damsté J. S. (1990) Organic sulphur compounds and other biomarkers as indicators of palaeosalinity. In *Geochemistry of Sulfur in Fossil Fuels* (Edited by Orr W. L. and White C. M.), pp. 417–443. Am. Chem. Soc., Washington.

Lotze F. (1957) *Steinsalt und Kalisalze.* Gebrüder Borntraeger, Berlin.

Risatti J. B., Rowland S. J., Yon D. A. and Maxwell J. R. (1984) Sterochemical studies of acyclic isoprenoids—XII. Lipids of methanogenic bacteria and possible contributions to sediments. *Org. Geochem.* **6,** 93–104.

Robinson N., Eglinton G., Brassell S. C. and Cranwell P. A. (1984) Dinoflagellate origin for sedimentary 4α-methyl-steroids and 5α (H)-stanols. *Nature* (*London*) **308,** 439–441.

Sinninghe Damsté J. S., Rijpstra W. I. C., de Leeuw J. W. and Schenck P. A. (1988) Origin of organic sulphur compounds and sulphur containing high molecular weight substances in sediments and immature crude oils. *Org. Geochem.* **13,** 593–606.

Sinninghe Damsté J. S., Eglinton T. I., Rijpstr W. I. C. and de Leeuw J. W. (1990) Molecular characterisation of organically-bound sulphur in sedimentary high-molecular-weight organic matter using flash pyrolysis and Raney Ni desulphurisation. In *Geochemistry of Sulfur in Fossil Fuels* (Edited by Orr W. L. and White C. M.), pp. 486–528. Am. Chem. Soc., Washington.

Sinninghe Damsté J. S., Betts S. E., Ling Y., Hofmann P. and de Leeuw J. W. (1993a) Hydrocarbon biomarkers of different lithofacies of the Salt IV Formation of the Mulhouse Basin, France. *Org. Geochem.* **20,** 1187–1200.

Sinninghe Damsté J. S., Keely B. J., Betts S. E., Bass M., Maxwell J. R. and de Leeuw J. W. (1993b) Variations in the abundances and distributions of isoprenoid chromans and long chain alkylbenzenes in sediments from the Mulhouse Basin: a molecular record of palaeosalinity. *Org. Geochem.* **20,** 1201–1215.

Sinninghe Damsté J. S., Hartgers W. A., Bass M. and de Leeuw J. W. (1993c) Characterization of high-molecular-weight organic matter in marls of the Salt IV Formation of the Mulhouse Basin. *Org. Geochem.* **20,** 1237–1251.

Sittler C. (1988) *Geol. Jahrbuch* **Reihe A, Heft 100,** 135.

Summons R. E., Volkman J. E. and Boreham C. J. (1987) Dinosterane and other steroidal hydrocarbons of dinoflagellate origin in sediments and petroleum. *Geochim. Cosmochim. Acta* **51,** 3075–3082.

Summons R. E., Thomas J. and Maxwell J. R. (1993) Secular and environmental constraints on the distribution of dinosterane in sediments and oils. *Geochim. Cosmochim. Acta* **56,** 2437–2444.

Thomas J. B., Marshall J., Mann A. L., Summons R. E. and Maxwell J. R. (1993) Dinosteranes (4,23,24-trimethylsteranes) and other biological markers in dinoflagellate-rich marine sediments of Rhaetian age. *Org. Geochem.* **20,** 91–104.

Volkman J. K. (1986) A review of sterol markers for marine and terrigenous organic matter. *Org. Geochem.* **9,** 83–99.

Volkman J. K. and Maxwell J. R. (1986) Acyclic isoprenoids as biological markers. In *Biological Markers in the Sedimentary Record* (Edited by Johns R. B.). Elsevier, Amsterdam.

Volkman J. K., Barrett S. M., Dunstan G. A. and Jeffrey S. W. (1993) Geochemical significance of the occurrence of dinosterol and other 4-methyl sterols in a marine diatom. *Org. Geochem.* **20,** 7–15.

Winters K., Parker P. L. and van Baalen Ch. (1969) Hydrocarbons of blue-green algae: geochemical significance. *Science* **163,** 467–468.

Waples D. W., Haug P. and Welte D. H. (1974) Occurrence of a regular C_{25} isoprenoid hydrocarbon in Tertiary sediments representing a lagoonal-type, saline environment. *Geochim. Cosmochim. Acta* **38,** 381–387.